



NUREG/CR-4778
ORNL/TM-10273

OAK RIDGE
NATIONAL
LABORATORY

MARTIN MARIETTA

Preliminary Studies of the
Morphology of Thermal Gradient
Tube Deposits from Fission Product
Release Experiments

S. J. Wisbey

Prepared for the
U.S. Nuclear Regulatory Commission
Office of Nuclear Regulatory Research
Under Interagency Agreement DOE 40-551-75

8805090156 880231
PDR NUREG
CR-4778 R PDR

OPERATED BY
MARTIN MARIETTA ENERGY SYSTEMS, INC.
FOR THE UNITED STATES
DEPARTMENT OF ENERGY

NOTICE

This report was prepared as an account of work sponsored by an agency of the United States Government. Neither the United States Government nor any agency thereof, or any of their employees, makes any warranty, expressed or implied, or assumes any legal liability or responsibility for any third party's use, or the results of such use, of any information, apparatus product or process disclosed in this report, or represents that its use by such third party would not infringe privately owned rights.

Available from

Superintendent of Documents
U.S. Government Printing Office
Post Office Box 37082
Washington, D.C. 20013-7982

and

National Technical Information Service
Springfield, VA 22161

NUREG/CR-4778
ORNL/TM-10273
Dist. Category R-3

Chemical Technology Division

PRELIMINARY STUDIES OF THE MORPHOLOGY OF THERMAL GRADIENT TUBE
DEPOSITS FROM FISSION PRODUCT RELEASE EXPERIMENTS

S. J. Wisbey*

*Guest scientist from AERE, Harwell, Didcot, Oxon OX11 0RA, England.

Manuscript Completed - December 1986
Date Published - March 1988

NOTICE This document contains information of a preliminary nature.
It is subject to revision or correction and therefore does not represent a
final report.

Prepared for the
U.S. Nuclear Regulatory Commission
Office of Nuclear Regulatory Research
Washington, DC 20555
under Interagency Agreement DOE 0551-0551-A1

NRC FIN No. B0453

Prepared by the
OAK RIDGE NATIONAL LABORATORY
Oak Ridge, Tennessee 37831
operated by
MARTIN MARIETTA ENERGY SYSTEMS, INC.
for the
U.S. DEPARTMENT OF ENERGY
under contract DE-AC05-84OR21400

ABSTRACT

Sections of thermal gradient tubes and deposits from filters that were used as collectors in several fission product release tests at Oak Ridge National Laboratory have been examined by scanning electron microscopy with elemental identification by energy dispersive X-ray analysis. The shape, size, and composition of the deposits are reported; correlations with experimental conditions, such as gas composition and temperature, as well as with independent analyses, have been made where possible. A wide variety of shapes and structures, apparently dependent on the deposition temperature, were photographed, and elemental analyses were recorded. Although some fission products (Cs, Ba, Ag) were detected, structural and impurity elements (Sn, Si, S, W, Pt) were predominant in most cases. Recommendations for conducting analytical procedures and handling similar samples are made for the future.

CONTENTS

| | <u>Page</u> |
|---|-------------|
| ABSTRACT | iii |
| LIST OF FIGURES | vii |
| LIST OF TABLES | ix |
| 1. EXECUTIVE SUMMARY | 1 |
| 2. INTRODUCTION | 1 |
| 3. OVERVIEW OF THE EXPERIMENTS | 2 |
| 4. SPECIMEN PREPARATION AND EXAMINATION | 5 |
| 5. EXPERIMENTAL DESCRIPTION AND PHOTOMICROGRAPHS | 9 |
| 5.1 HS-2 (SIMULANT FUEL HEATED TO 2000°C AND 2400°C) | 9 |
| 5.1.1 Experimental Details | 9 |
| 5.1.2 Photomicrographs | 9 |
| 5.2 HS-4 (SIMULANT FUEL HEATED TO 2000°C AND 2450°C) | 20 |
| 5.2.1 Experimental Details | 20 |
| 5.2.2 Photomicrographs | 20 |
| 5.3 HI-6 (HIGH-BURNUP FUEL HEATED TO 2000°C) | 26 |
| 5.3.1 Experimental Details | 26 |
| 5.3.2 Photomicrographs | 28 |
| 5.4 VI-1 (HIGH-BURNUP FUEL HEATED TO 1750°C AND 2030°C) | 31 |
| 5.4.1 Experimental Details | 31 |
| 5.4.2 Photomicrographs | 32 |
| 5.5 VI-2 PRETEST (FURNACE HEATED TO 1725°C) | 39 |
| 5.5.1 Experimental Details | 39 |
| 5.5.2 Photomicrographs | 39 |
| 6. DISCUSSION | 41 |
| 7. CONCLUSIONS AND RECOMMENDATIONS | 44 |
| 8. REFERENCES | 46 |

LIST OF FIGURES

| <u>Number</u> | | <u>Page</u> |
|---------------|---|-------------|
| 1 | Vertical fission product release apparatus | 3 |
| 2 | Collection train and effluent analyzing system used in the fission product release tests | 4 |
| 3 | Temperature and fission product release history for test HS-2 | 10 |
| 4 | Posttest view of the simulated fuel specimen used in test HS-2 | 11 |
| 5 | SEM photomicrographs of surface deposits examined at 1 cm, (a) and (b), and 9 cm, (c) and (d), into TGT A (test HS-2) ... | 13 |
| 6 | SEM photomicrographs of surface deposits examined at 22 cm, (a), and 28 cm, (b), into TGT A (test HS-2). Photomicrographs (c) and (d) were aerosol deposit taken from the train "A" prefilter (test HS-2) | 14 |
| 7 | SEM photomicrographs of surface deposits examined near the inlet end (1 cm) of TGT B (test HS-2) | 16 |
| 8 | SEM photomicrographs of surface deposits 8 cm, (a) and (b), and 16 cm, (c) and (d), into TGT B (test HS-2) | 17 |
| 9 | SEM photomicrographs of surface deposits examined at 24 cm, (a) and (b), into TGT B (test HS-2). Aerosol deposit from the train "B" prefilter is shown in (c) and (d) | 18 |
| 10 | Posttest view of the simulated fuel specimen used in test HS-4 | 21 |
| 11 | SEM photomicrographs of surface deposits at 3 cm into TGT A (test HS-4) | 22 |
| 12 | SEM photomicrographs of surface deposits examined at 16 cm, (a) and (b), and 28 cm, (c), into TGT A (test HS-4). Aerosol deposit from the train "A" prefilter is shown in (d) | 24 |
| 13 | SEM photomicrographs of surface deposits at 2 cm, (a) and (b), and 14 cm, (c) and (d), into TGT B (test HS-4) | 25 |
| 14 | SEM photomicrographs from test HS-4 of surface deposits at 32.5 cm, (a), into TGT B and of aerosol deposits from train B, (b) | 27 |

| <u>Number</u> | | <u>Page</u> |
|---------------|---|-------------|
| 15 | SEM photomicrographs of deposits from the entrance region (a) and ~1 cm (b) into the TGT (test HI-6) | 29 |
| 16 | SEM photomicrographs of surface deposits examined at 16 to 18 cm, (a) and (b), 32 cm, (c), and of an unheated but leached material (test HI-6) | 30 |
| 17 | SEM photomicrographs of surface deposits at the inlet end, (a) and (b), and 11 cm, (c), into TGT A (test VI-1). The view in (d) shows the surface at 11 cm after it was leached in basic and acidic leaches | 33 |
| 18 | SEM photomicrographs of surface deposits at 11 cm, (a), and 16 cm, (c) and (d), into TGT A (test VI-1). The view in (b) shows the surface at 11 cm after it was leached in basic and acidic leaches | 34 |
| 19 | SEM photomicrographs of surface deposits at the inlet region of TGT B (test VI-1) | 35 |
| 20 | SEM photomicrographs of surface deposits examined at the outlet end, (a) and (b), of TGT B and the inlet end, (c) and (d), of TGT C (test VI-1) | 37 |
| 21 | SEM photomicrographs of surface deposits at 6 cm, (a) and (b), and 15 cm, (c), into TGT C (test VI-1). The view in (d) shows the surface at 15 cm after it was leached in basic and acidic leaches | 38 |
| 22 | SEM photomicrographs of surface deposits at 1 cm, (a), 6 cm, (b), 15 cm, (c), and 36 cm, (d), into the TGT used in pretest VI-2 | 40 |

LIST OF TABLES

| <u>Number</u> | | <u>Page</u> |
|---------------|--|-------------|
| 1 | Details and results of fission product release tests from which samples were studied by SEM/EDX | 6 |
| 2 | X-ray emission energies of elements found in fission products, cladding, and structural materials, as determined by SEM/EDX analysis | 8 |
| 3 | Summary of relative X-ray intensities observed in various SEM/EDX samples | 19 |

PRELIMINARY STUDIES OF THE MORPHOLOGY OF THERMAL GRADIENT TUBE
DEPOSITS FROM FISSION PRODUCT RELEASE EXPERIMENTS

S. J. Wisbey

1. EXECUTIVE SUMMARY

Material that vaporized from irradiated and simulant fuel specimens during fission product release experiments was collected on platinum thermal gradient tubes (TGTs) and glass fiber filter surfaces. Samples from these tubes and filters have been examined by scanning electron microscopy to determine the elemental composition and morphology of the deposits. A large range of shapes and sizes was evident; complex interactions occurred between volatile species and the surfaces. Temperature, gas composition, and contaminants from the furnace ceramics all affected the physical features on the surface. Larger particles, more firmly attached to the surface, were located at the hottest ends of the TGTs. In the cooler regions, the deposited particles were smaller and less tightly held. Although the TGTs contained single particles in the diameter range of 0.1 to 50 μm , the filter surfaces were universally covered with very fine particles ($<0.1 \mu\text{m}$). Cesium was identified at most positions examined; discrete cesium-containing crystals were observed only in a tube that had operated under chemically reducing conditions. Tin was a major constituent of most deposits, and uranium, probably released as spalled particles, was found occasionally. When silver control rod alloy was heated with the fuel rod, a range of silver-, indium-, and cadmium-containing structures was observed in the tubes. The presence of sulfur and silicon as contaminants led to complications of interpretation, as they alloyed and reacted with the platinum substrate.

2. INTRODUCTION

The release of fission products from overheated fuel in severe reactor accidents is a subject of continuing study around the world. A long-term program at Oak Ridge National Laboratory (ORNL) has focused on light-water reactor (LWR) fuel in a series of tests in which simulant and irradiated fuel specimens have been heated to temperatures of up to 2400°C (2675 K) in flowing-steam atmospheres. Fission products and structural materials that were released from the specimens have been collected in TGTs and on filters in order to separate chemical species by their condensation profiles. These tubes have been lined with noble metals, such as platinum, or occasionally, more "realistic" materials, such as Inconel and stainless steel. Many reports have been published describing experimental conditions and results obtained from these tests.¹⁻⁷ Most of the analysis of TGT deposits has been by gamma-ray spectrometry, spark-source mass spectrometry (SSMS), or examination of solutions used to leach species from the metal surfaces. The present study has taken a more direct look at the deposits by using scanning electron microscopy (SEM) to examine the surfaces directly in the hope of understanding something of the morphology and deposition characteristics of the species released from the fuel specimens. Samples of TGTs from a range of tests have been

studied, and the resulting photographs have been used in conjunction with other analytical data to correlate observations with experimental conditions wherever possible.

3. OVERVIEW OF THE EXPERIMENTS

The continuing series of fission product release experiments at ORNL has, at various times, used commercially irradiated fuel, simulant fuels, and individual, simulated radioactive fission product tracers, or their compounds, to study the extent and form of releases from fuel. The fuel specimens were heated in induction furnaces at temperatures of up to 2450°C (2725 K) in flowing-steam atmospheres. The current, vertical design of the furnace used is shown in Fig. 1. Previous experiments utilized a similar design in a horizontal orientation.¹ As species are released from the fuel, they exit the Zircaloy cladding through a small hole, which is drilled for that purpose (to prevent ballooning or bursting of the clad during heatup), or through cladding fractures or molten regions and are swept into a TGT and eventually to a series of filters. The components of the system for fission product collection and effluent analysis are depicted in Fig. 2. The TGTs are designed to collect the volatile species, which condense from the flowing carrier gas and deposit on the surface as their saturated vapor pressure is exceeded. The TGTs are heated to ~900°C (1175 K) at their inlet and ~200°C (475 K) at their exit. These tubes are normally lined with platinum foil, as an inert surface, but stainless steel and/or Inconel tubes have been used. The temperature of the TGT is measured on the outside of a quartz or Inconel tube, which contains the platinum liner, using thermocouples; the TGTs are heated externally to maintain the required temperatures. However, the temperature of the gas passing through the tube will be higher than that measured on the outside wall. Near the inlet, there may be a greater difference than at the exit. The first exterior thermocouple is located ~0.5 cm downstream of the entrance to the platinum liner, and temperatures in the gas in this region may be as much as 200°C higher than those recorded by the first thermocouple.² It is hoped that these differences can be measured in the future, as they may have a significant impact on TGT behavior. In a real reactor system, the pipe work and above-core structure of the primary system may be in contact with similarly hot gas flows and the temperatures to be expected are an important feature of this work. As the test series has progressed, experimental variables have included fuel temperature, ramp rate, time at maximum temperature, and steam flow rate. Recent modifications have included the introduction of two and then three TGTs in parallel such that the flow out of the fuel region can be directed through fresh tubes during an experiment. Data can therefore be obtained as a function of time and fuel temperature, as well as of other conditions.

The gas entering the fuel region consists of helium and steam. As the temperature exceeds 1100°C (1375 K), a steam/Zircaloy reaction begins, liberating hydrogen and producing ZrO₂ from the metallic zirconium. At its peak rate, this reaction removes most of the steam from the gas (steam starvation) and the gas exiting the furnace will be a He/H₂ mixture

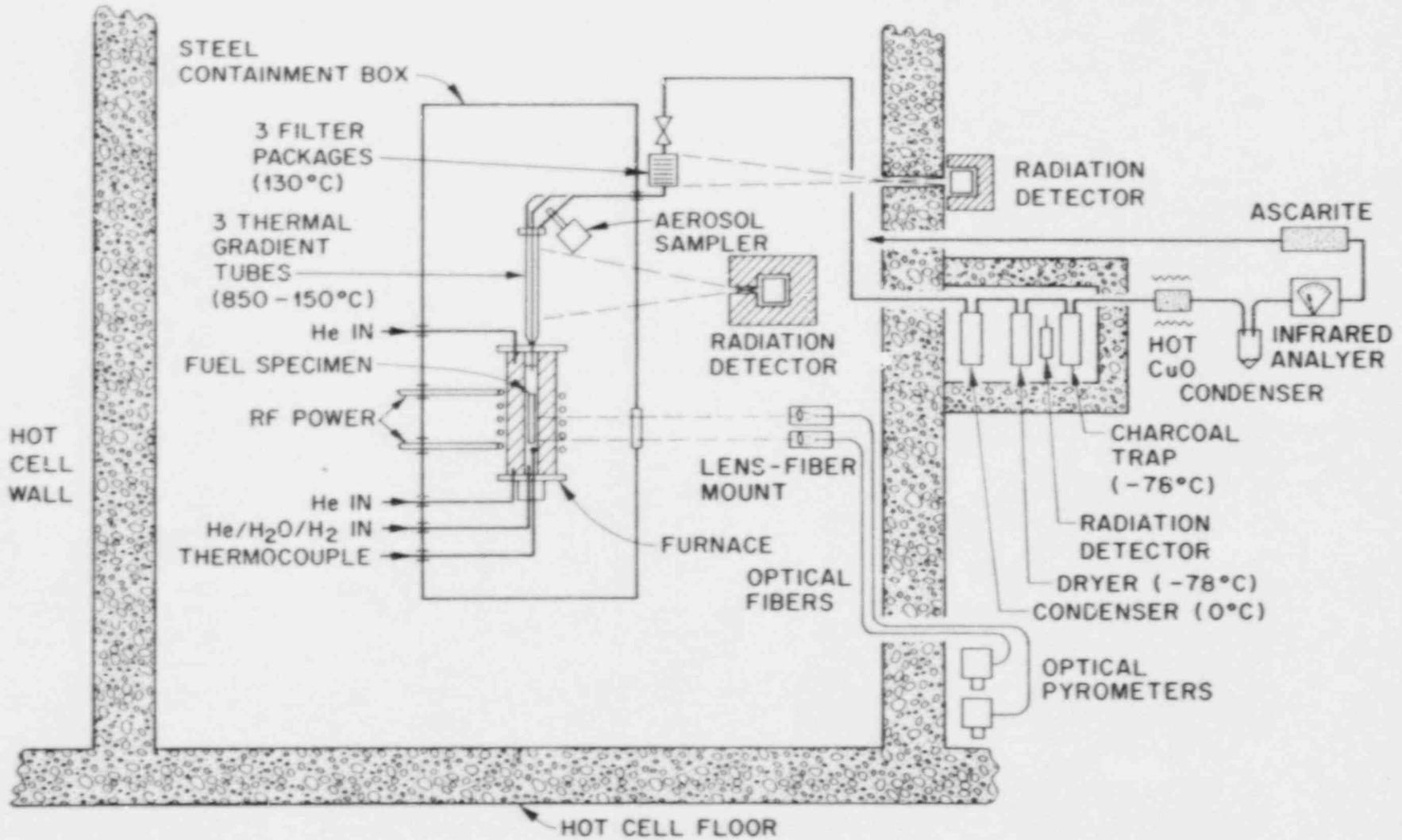


Fig. 1. Vertical fission product release apparatus.

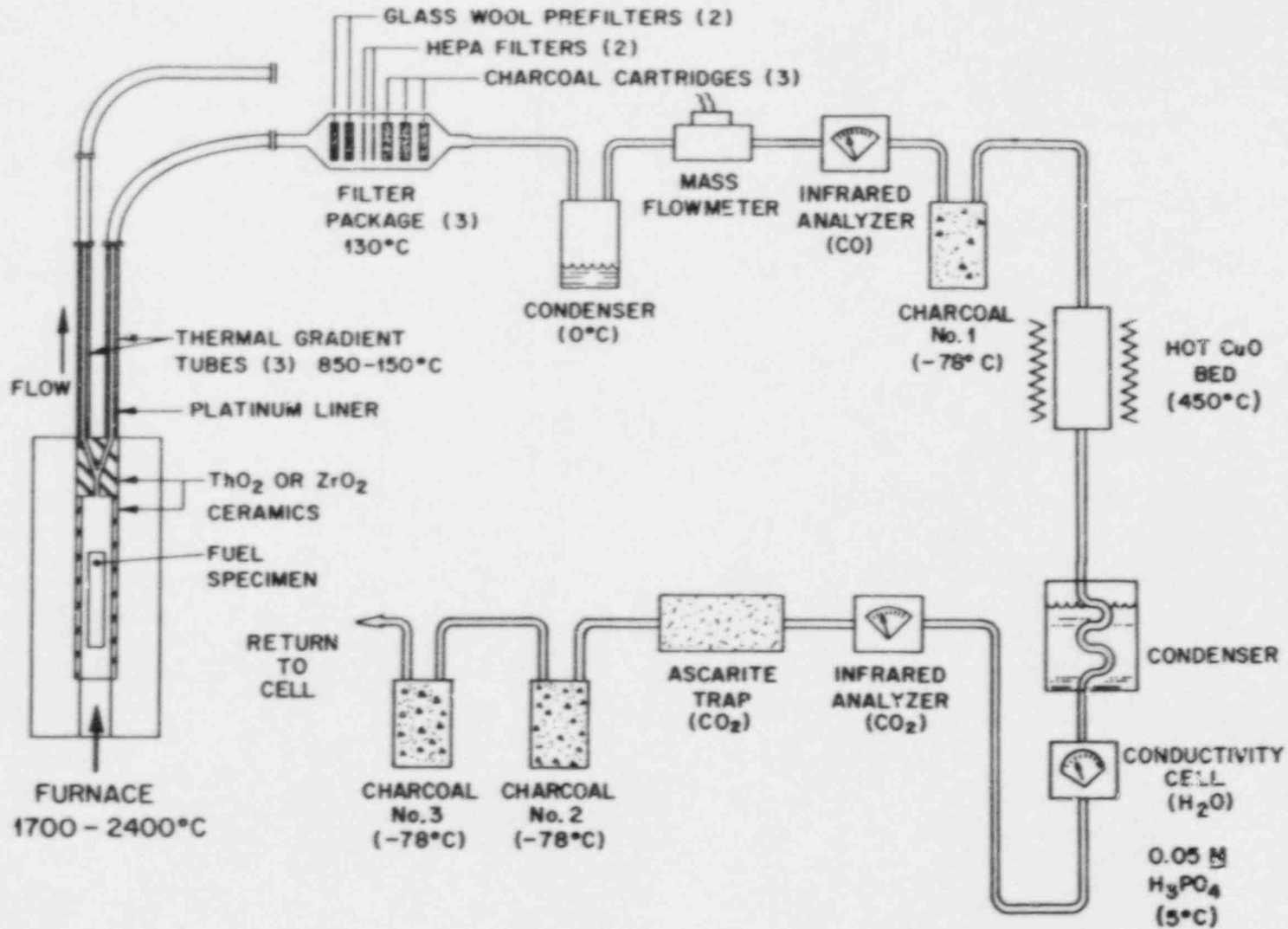


Fig. 2. Collection train and effluent analyzing system used in the fission product release tests.

only. Later, when Zircaloy oxidation is nearing completion, some steam will escape the furnace, and finally, at complete oxidation, no steam will be consumed. This progression can be calculated using various oxidation rate models, and this will be discussed in detail for the specific experiments described below. The composition of the gas exiting the fuel is important in that oxidizing and reducing conditions may influence speciation and deposition behavior in the TGTs. Other gases may be present due to steam leakage into the furnace ceramics that surround and insulate the fuel region. The major products of this leakage are H_2 and CO from the steam reaction with the graphite susceptor; other contaminants were released from the ceramics, such as compounds of P, S, and Si.

The species released from the fuel region may condense to form aerosols before they reach the TGTs and may subsequently be deposited on the TGT surface or be swept through to the filters. One important aerosol component is tin from the Zircaloy cladding; other possible aerosol producers include the control-rod material (e.g., Ag-In-Cd rods for PWRs and B_4C for BWRs) and structural materials (e.g., Fe, Cr, Ni, Mn, Co) from stainless steels and other metallic components. These have been, or will be, included in the test series. The species may also condense directly onto fixed surfaces, such as the ceramics in the furnace or platinum in the TGTs. This occurs as their saturated vapor pressure is exceeded at the temperature of the surface.

Analysis of these experiments has normally included visual observations, gamma-ray spectrometry of fuel and all test components, and SSMS of deposits taken directly from the TGTs and filters and of samples of solutions used to leach fission product species from the tubes. Iodine and, occasionally, tellurium have been identified by neutron activation analysis after chemical separation from interfering elements. The individual tests from which small samples of TGTs have been studied by scanning electron microscopy (SEM) are described below, with some of the experimental details and test results shown in Table 1.

4. SPECIMEN PREPARATION AND EXAMINATION

The instrument used in this study was an ISI Alpha 9 SEM with a 15-kV accelerating voltage. The instrument was unmodified and was used in an open laboratory; a "Kevex" system energy dispersive X-ray (EDX) analyzer was attached to the instrument, which allowed the qualitative study of the average elemental composition of the area under observation for elements with atomic numbers >11 . Due to the low accelerating voltage, no spectral lines above 15 keV could be detected.

Specimens from TGTs were mounted on standard aluminum stubs, usually by double-sided tape. Silver paint was sometimes used to disperse the charge buildup. The TGT sections were usually no more than 0.5 cm in any dimension and triangular, which allowed for orientation to be easily identified once the image had been obtained and reduced the amount of material in the microscope. The latter point was important because some of the samples (especially those from VI-1) were highly radioactive, and

Table 1. Details and results of fission product release tests from which samples were studied by SEM/EDX

| | Test | | | |
|---|-----------------------|-------------------------|------------------|------------|
| | HS-2 | HS-4 | HI-6 | VI-1 |
| Date conducted | 6/11/84 | 10/18/84 | 12/14/83 | 12/17/85 |
| Fuel type | Simulant ^a | Simulant ^{a,b} | Irradiated | Irradiated |
| Maximum temperature during test, °C | >2425 | >2450 | ~2000 | 2050 |
| Time above 1700°C, min | 32 | 34 | 6 | 53 |
| TGT material (No.) | Pt (1) | Pt (2) | SS (1) | Pt (3) |
| Orientation of test | Horizontal | Horizontal | Horizontal | Vertical |
| Steam flow, L/min | 1.34 | 1.30 | 3.0 ^c | 1.5 |
| Complete Zircaloy oxidation | No | No | No | Yes |
| Fission products released from furnace, % | | | | |
| Kr | | | 29.6 | 57.4 |
| Cs | | | 33.1 | 74.3 |
| I | | | 24.7 | 33.0 |
| Te | | | | |
| Sb | | | | 28.0 |
| Ag | | 61.7 ^d | | 33.2 |
| Ru | 9×10^{-3} | 0 ^e | | |
| Eu | 4×10^{-3} | 5×10^{-4} | | |

^aSimulant fuel was supplied by KfK, West Germany, and contained ^{103}Ru and ^{154}Eu tracers, as described by Schreibermaier et al., in Herstellung von Kernbrennstoff mit Simuliertem Abbrand (Fission) an der Anlage FIFa, KfK-2991, Kernforschungszentrum Karlsruhe, June 1980.

^bPlus a stainless-steel-clad Ag-In-Cd-Sn rod, and a stainless steel rod, both slightly irradiated to produce radiotracers: $^{110\text{m}}\text{Ag}$, ^{51}Cr , ^{54}Mn , ^{59}Fe , and ^{60}Co .

^cInitial rate; declined during test.

^dFrom Ag-In-Cd-Sn control rod.

^eDecay time too long for accurate measurement.

the possibilities of operator exposure and instrument contamination had to be reduced as much as possible. (To further reduce the contamination threat and provide a static-free picture, gold-layer coating is recommended. Unfortunately, this option was not available during this study, but it should be used in any future work of this type.)

The selection of samples was normally aided by study of the gamma scans of the TGTs (VI-1). These showed regions of higher activity that might prove interesting. In the absence of this type of information (HS-2, HS-4), samples were cut from the tubes at three or four points, covering a range of TGT temperatures from the inlet ($\sim 900^{\circ}\text{C}$) to near the outlet ($\sim 200^{\circ}\text{C}$). This part of the work was conducted in a fume hood, and care was taken to avoid the spread of contamination to the aluminum stub and surrounding areas. Study of the deposits was done in a standard way. General observation over the whole surface, at low magnifications (up to $100\times$), was followed by detailed study of the deposit's structure and any unusual outcrops or formations. X-ray spectra were recorded, and photographs of the structure were taken at several magnifications, usually $400\times$, $2000\times$, and $5000\times$. Due to the large depth of field in an SEM, the real magnification of these photographs was adjusted by a working distance factor, usually in the range of 0.58 to 0.62, depending on the exact positioning of the sample. The exact scaling is recorded with each of the micrographs in the figures. To allow for more accurate comparisons of samples, it is important to use similar magnifications between samples.

The vacuum chamber of the SEM was always carefully checked for contamination after a sample was removed. A small amount of contamination was discovered after the study of a section from the cooler end of a VI-1 TGT. The bonding of the deposits to each other and to the platinum surface was reduced at the lower temperatures; this problem may be overcome by the gold coating. Even with the highest-activity samples (~ 0.5 R/h at contact), very low dose rates were detected outside the chamber (~ 10 mR/h) and there was no noticeable effect on the image quality from the high levels of β radiation. The radiations did, however, introduce a background response to the X-ray spectra that was highest at the low energies and tailed off at higher energies. The tail extended beyond 15 keV and usually contained a few small peaks, which are artifacts of the interaction of radiation (mostly from ^{137}Cs) with other materials in the system, especially the platinum base. They must not be confused with responses from the deposits themselves. When studying a high-activity sample, it was necessary to record a background X-ray spectrum with the beam turned off. This was then compared with a spectrum obtained with the beam on to identify and then ignore these artifact peaks.

There are several limitations to the use of an SEM as an analytical tool. Most importantly, the X-ray analysis can only give an average elemental composition for the area under examination. Elements present at $<0.1\%$ will only rarely be visible in the spectrum. The response from the surface comes from the whole of the area being scanned, up to $2\ \mu\text{m}$ deep.

Hence, peaks due to the platinum base were present in all but the analysis of the thickest deposits. Several X-ray peaks overlap, and it was difficult to separate contributions from various elements. Some of these interactions are shown in Table 2. Important areas are P/Zr/Pt, S/Mo, U/Cd, and the elements from Ag through Ba, where small amounts of one in the presence of another were difficult to interpret. This was especially true for pairs such as Ag/In, Cs/Ba, and Te/I, which have very similar atomic numbers. Finally, the X-ray analysis could not unambiguously tell anything about the chemical form of the elements. Sometimes this was inferred from the available evidence; however, elements with $Z < 11$ cannot be detected with the system used. Despite these limitations, useful and important results were obtained even with this simple system. Moreover, the instrument and the techniques developed should provide opportunities for useful studies of TGT deposits in future fission product release tests.

Table 2. X-ray emission energies of elements found in fission products, cladding, and structural materials as determined by SEM/EDX analysis

| Element | Primary X-ray energy (keV) | Other useful X-ray energies (keV) |
|---------|-------------------------------|--------------------------------------|
| Si | 1.740 | |
| W | 1.775 | 8.396 |
| P | 2.013 | |
| Zr | 2.042 | 15.772 |
| Pt | 2.050 | 9.441 |
| Mo | 2.293 | 17.476 |
| S | 2.307 | |
| Ag | 2.984 | 22.159 |
| Cd | 3.133 | 23.170 |
| U | 3.170 | 13.612 |
| In | 3.286 | 24.206 |
| Sn | 3.443 | 25.267 |
| Sb | 3.604 | 26.355 |
| Te | 3.769 | 27.468 |
| I | 3.937 | 28.607 |
| Cs | 4.286 | >30 |
| Ba | 4.465 | >30 |

5. EXPERIMENTAL DESCRIPTION AND PHOTOMICROGRAPHS

5.1 HS-2 (SIMULANT FUEL HEATED TO 2000°C AND 2400°C)

5.1.1 Experimental Details

The HS-series consisted of four tests with simulant fuels that were produced in the Federal Republic of Germany and contained fission product tracers.^{3,4} Tests HS-1 and HS-3 contained the more volatile fission product species (Cs, I, Te), and the pellets were pressed into shape without being sintered. These pellets cannot be described as exhibiting real fuel behavior. Tests HS-2 and HS-4, however, contained less volatile fission product species, and the pellets were sintered at 1500°C. The added fission products were Ru (¹⁰³Ru traced), Mo, Eu₂O₃ (¹⁵⁴Eu traced), ZrO₂, BaO, and CeO₂. The pellets were loaded into Zircaloy tubes (18 cm long) with normal UO₂ pellets at the ends; Zircaloy end caps were welded into place. A small hole was drilled through the end cap downstream from the gas flow, and the fuel specimen was heated in the horizontally oriented furnace at 2000°C for 10 min and then at 2400°C for another 10 min. The gas flow was directed through TGT A until the temperature was increased above 2000°C. The flow was then directed through TGT B throughout the higher-temperature phase and during cooldown of the fuel (see Fig. 3).

Observation of the fuel specimen after the test indicated that some of the Zircaloy had melted. The thorium boat and tube in which the sample was contained had softened and deformed (Fig. 4). Calculations of steam oxidation of Zircaloy in this test indicate that, with no melting, the cladding should have oxidized completely shortly after reaching the maximum temperature. Beyond this time, only 10% of the steam was converted to hydrogen, due to continued oxidation of the end caps, which were much thicker than the cladding. They should not have exceeded 70% oxidation at the end of the test. Melting must have occurred at low oxidation and high temperature (>1800°C). This may have delayed the completion of oxidation by forming a relatively thick liquid pool and may have maintained the hydrogen level at a higher value than predicted for a longer time. Calculations using a simple melt model, in which the geometry of the cladding changes at the Zircaloy melt temperature, indicated that steam starvation occurred for more than 10 min but that full oxidation of all Zircaloy was still achieved on reaching the maximum temperatures.⁵ A small amount of Zircaloy interaction with the uranium pellets was observed, and a total material release to TGTs and filters of 1.166 g was recorded. However, very little of the traced ruthenium and europium was released from the furnace region (<10⁻²% in both cases).

5.1.2 Photomicrographs

Specimens were taken from the two TGTs that had not been leached and mounted for analysis in the SEM as described in Sect. 4 above. Samples were taken from TGT A at 1 cm (~820°C), 9 cm (700°C), 22 cm (430°C), and 28 cm (330°C) and from the TGT B at 1 cm (~830°C), 8 cm

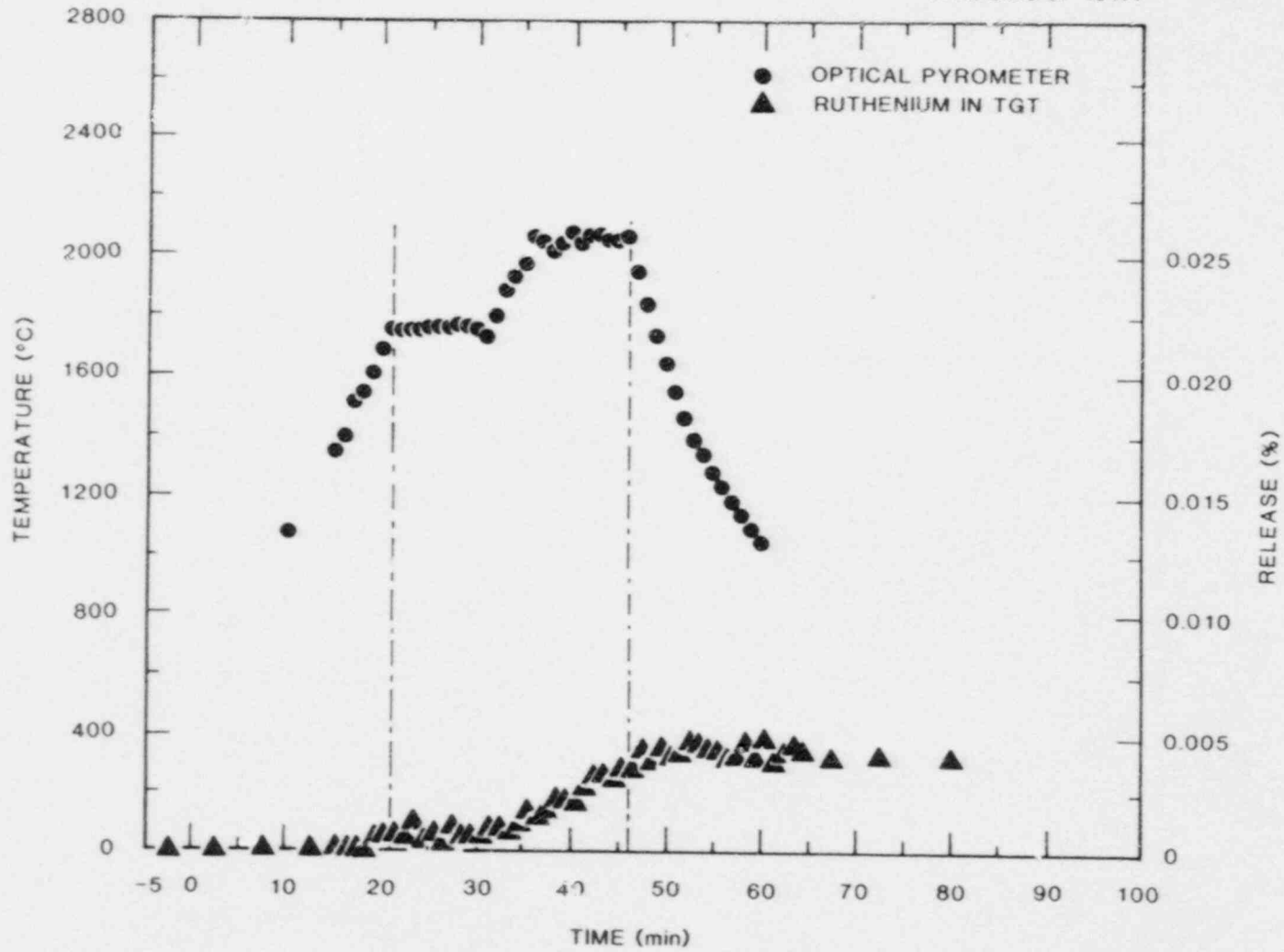


Fig. 3. Temperature and fission product release history for test HS-2.

ORNL-PHOTO 4021-84

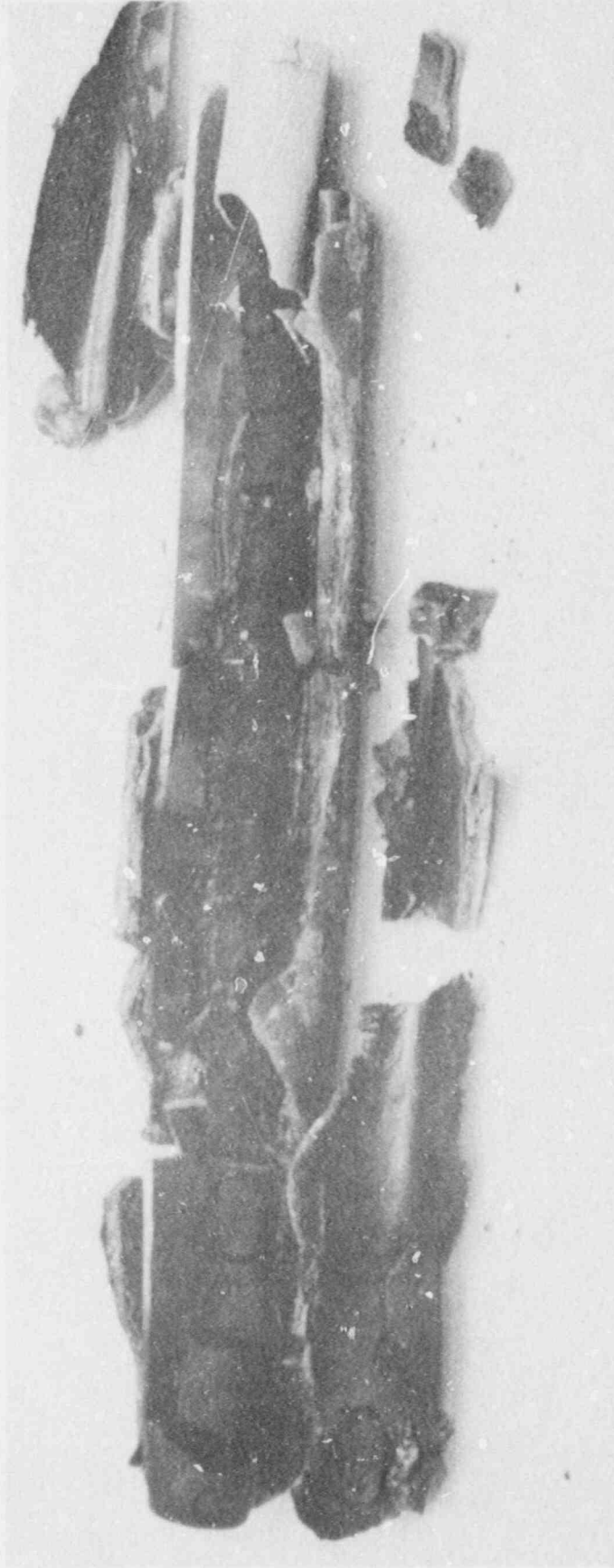


Fig. 4. Posttest view of the simulated fuel specimen used in test HS-2.

(730°C), 16 cm (550°C), and 24 cm (360°C). Samples were also taken from the two glass wool prefilters (both at ~150°C).

As there were no volatile fission products in this sample, the releases from the fuel region were dominated by tin. Some of the thermocouple material was also released after the ceramic thimble cracked and allowed oxidation; tungsten was detected in both TGTs A and B. Uranium was found in some samples, as were Ba, Fe, and S. Only a limited amount of analytical work was conducted on HS-2, and there are subsequently very few independent analyses for comparison.

Figure 5 (a) and (b) shows photomicrographs of surface deposits examined at 1 cm into TGT A. Samples taken close to the entrance region showed extensive cracking in the deposits. All samples taken from the first 3 cm or so of platinum TGTs examined in this report were brittle and were difficult to cut and lay flat. Some of the large cracks in the low-magnification pictures were due to this brittleness. The grain boundaries had been attacked and contained some tin. Discrete particles containing tungsten were also found. Overall, the deposits were quite thin and contained a range of particle sizes and shapes, down to $<0.5 \mu\text{m}$ in diameter.

At 9 cm into TGT A [Fig. 5 (c) and (d)], the deposits were rather smooth, obscuring the platinum surface structure. Again, tin was the major material found on the surface, apart from platinum. It appeared from the circles [Fig. 5 (d)] that some liquid arrived on the surface and "dried out." A possible explanation is the deposition of liquid tin, which has a vapor pressure of 2.7×10^{-6} Pa at 700°C; the "drying out" could involve formation of an alloy with the platinum surface.

At 22 cm into TGT A [Fig. 6 (a)], the platinum surface was found to be covered with $\sim 1\text{-}\mu\text{m}$ particles. These contained a lot of Sn, with some Si, Cr, and Fe. The deposits were quite thick, weakening the signal from the platinum substrate. These particles probably condensed in the gas phase and deposited onto the surface as aerosols.

At 28 cm into TGT A [Fig. 6 (b)], there was a thick, loosely packed deposit, not unlike fresh snow or candy floss, which had poor adhesion to the platinum substrate and very high porosity. The deposit contained very high levels of tin, with smaller amounts of silicon and sulfur from the ceramics in the furnace. The tin was probably an oxide: macroscopically, the sample had a dull white coating. This material would be readily resuspended by flowing gases or liquids.

Material collected on the filter beyond TGT A [Fig. 6 (c) and (d)] was composed of very small primary particles, $\sim 0.1 \mu\text{m}$ or less, which were tightly packed and came off in sheets. It was composed almost entirely of tin, probably as the oxide.

The material in TGT B was quite different, especially near the inlet end. The temperature in the furnace region was at 2400°C, and the deposits

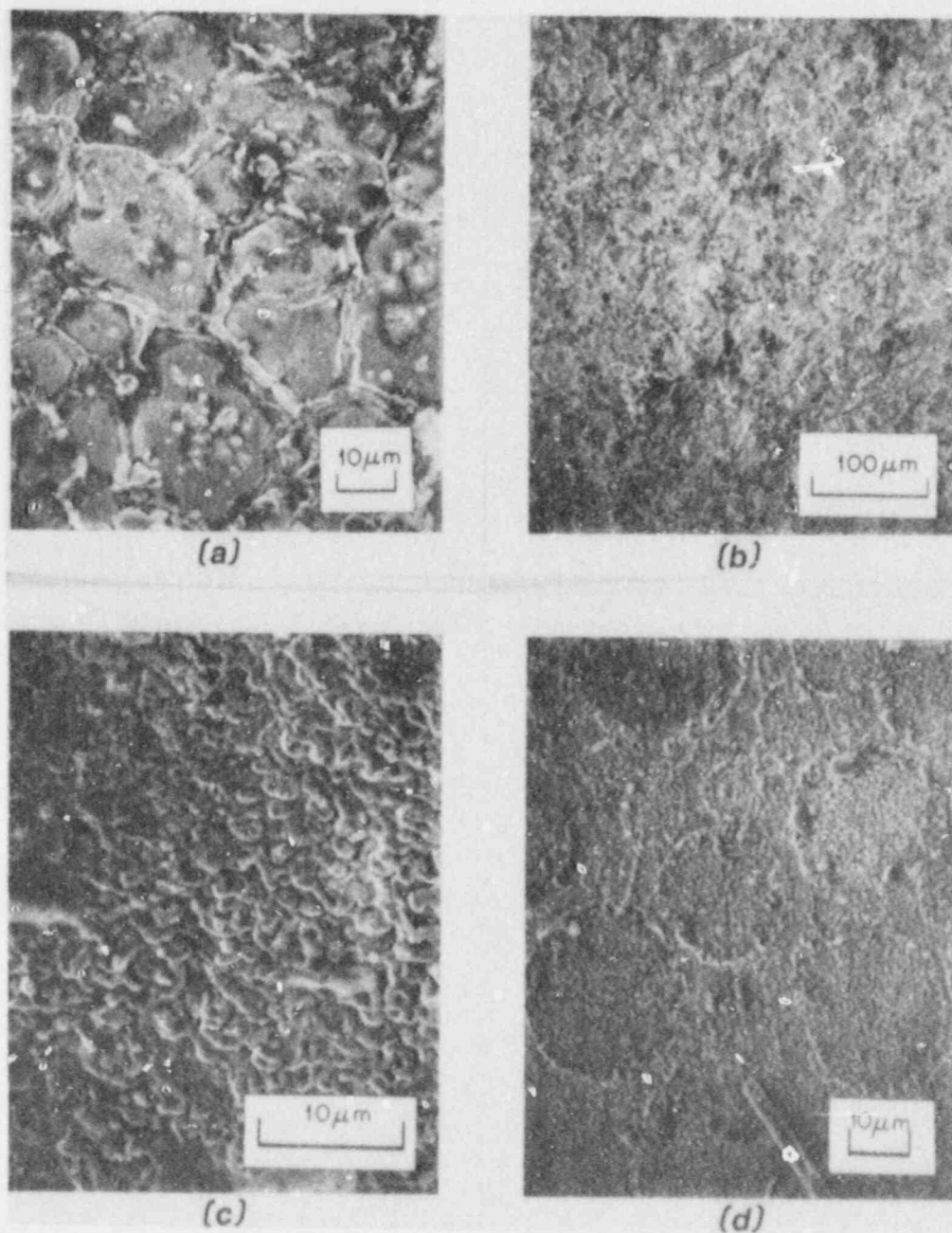


Fig. 5. SEM photomicrographs of surface deposits examined at 1 cm, (a) and (b), and 9 cm, (c) and (d), into TGT A (test HS-2).

ORNL-PHOTO 317-86

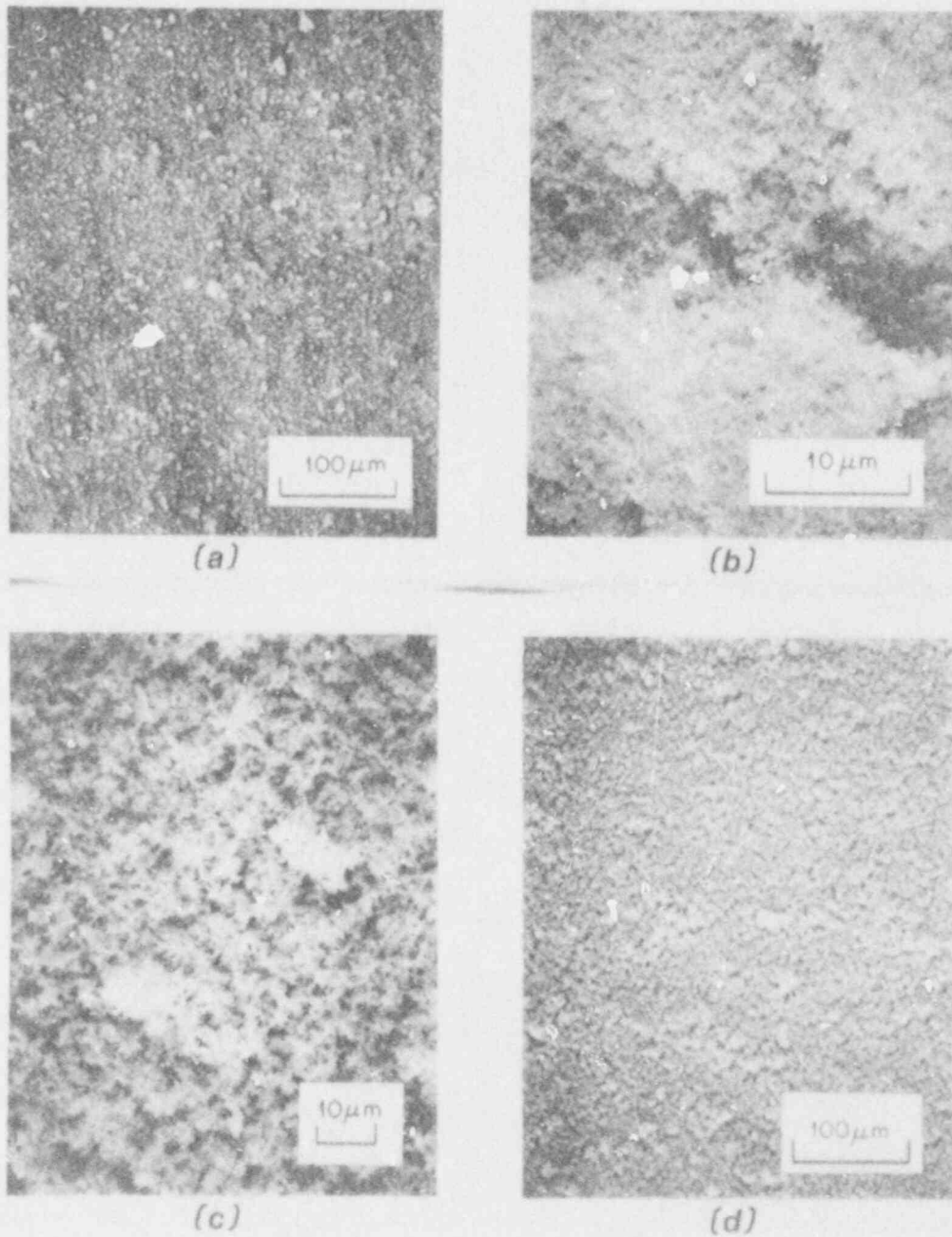


Fig. 6. SEM photomicrographs of surface deposits examined at 22 cm (a), and 28 cm (b), into TGT A (test HS-2). Photomicrographs (c) and (d) were aerosol deposit taken from the train "A" prefilter (test HS-2).

at 1 cm (Fig. 7) were both thicker and more clearly crystalline than in TGT A. Extensive, deep cracking in the deposits occurred on handling the platinum. Tin was the major constituent, with localized concentrations of tungsten and small amounts of uranium also visible. Surface deposits of more porous material [Fig. 7 (d)] contained concentrations of uranium. However, uranium was essentially absent in the lower (earlier release) layers. The platinum signal was reduced due to the thickness of the deposits.

At 8 cm into TGT B [Fig. 8 (a) and (b)], the surface retained a crystalline, altered appearance. The platinum signal was repressed, and tin and tungsten made up the bulk of the surface layer. There was further evidence of uranium transport: several isolated concentrations were located on top of the main deposit. Some were quite porous and fluffy, while others were more crystalline in appearance. Where some of the surface layer had been lost, platinum and tin gave high signals, and a deposit similar to that found near this temperature in TGT A was seen.

At 16 cm into TGT B [Fig. 8 (c) and (d)], the deposits were much more porous but appeared to have a crystalline nature of their own, with less interaction with the platinum substrate. The platinum signal was severely repressed, indicating a thick layer. Tin and tungsten dominated the deposits, but uranium was also featured and concentrations of sulfur and barium were detected, although not always together. Some of the fine coral-like deposits were quite rich in uranium. These deposits probably left the fuel as vapor and condensed onto the platinum surface.

The final sample from TGT B, at 24 cm [Fig. 9 (a) and (b)], showed a tightly packed layer of fine ($<0.5 \mu\text{m}$) particles, with little evidence of interaction with the platinum surface. The surface structure was quite porous and tended to flake off in sheets. The platinum signal was severely repressed, and the deposit was composed largely of tin, with some uranium and tungsten. There was no evidence of barium or other elements.

The glass wool prefilter material was similar to that found beyond the TGT A [Fig. 9 (c) and (d)]. The primary particles were very small ($<0.1 \mu\text{m}$ diameter) and were packed into thick sheets that flaked off in lumps of $\sim 0.1 \text{ mm}$. The major constituents of the deposits on the filter were Sn, W, and U, with smaller amounts of Ba and Fe. A response was also obtained in the P/Zr/Pt region of the X-ray spectrum, but it was impossible to separate these elements. This may indicate transport of zirconium cladding or platinum from the tubes.

A summary of the relative X-ray intensities of various elements, as recorded by EDX analysis for all samples in this report, is presented in Table 3.

ORNL-PHOTO 318-86

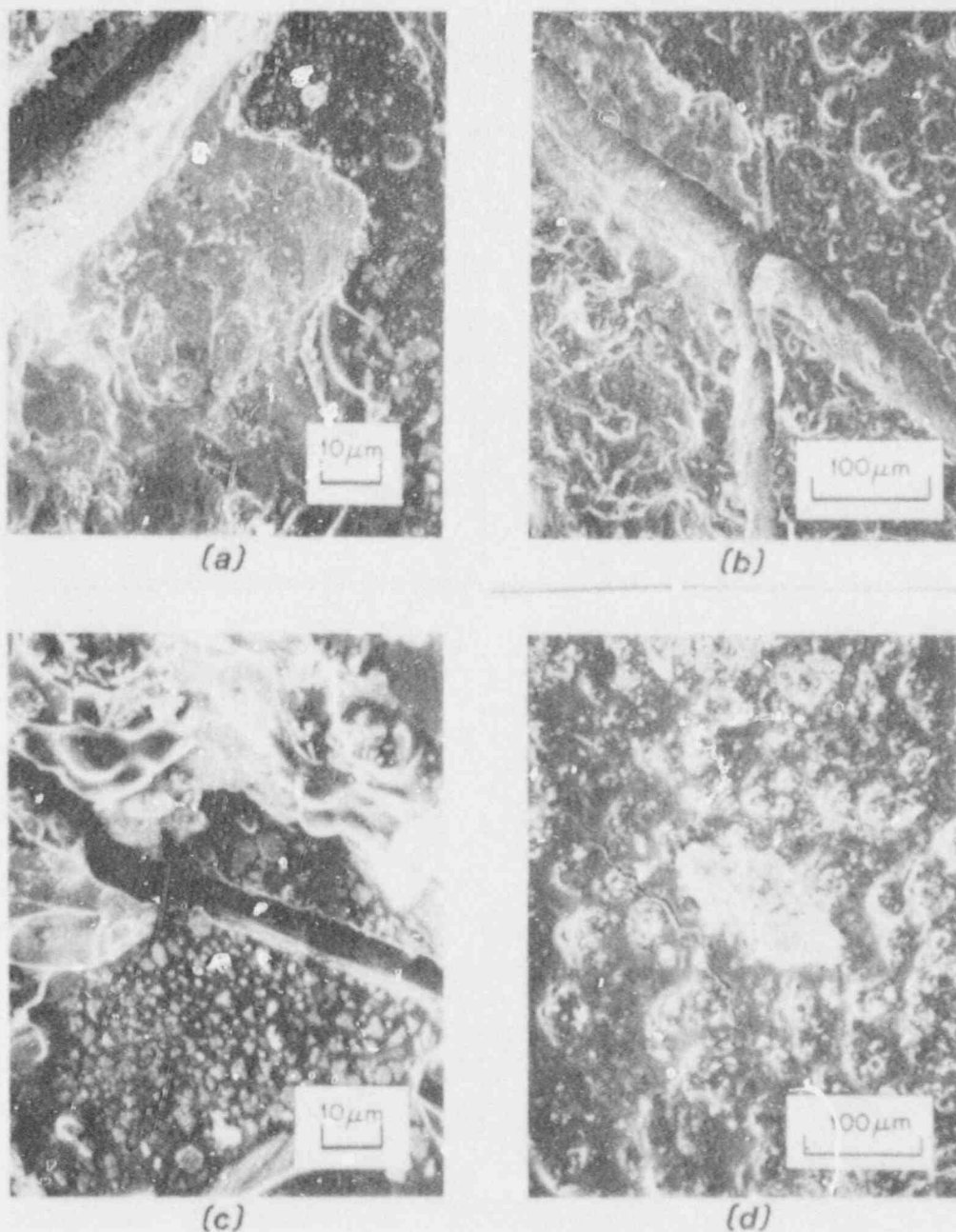


Fig. 7. SEM photomicrographs of surface deposits examined near the inlet end (1 cm) of TGT B (test HS-2).

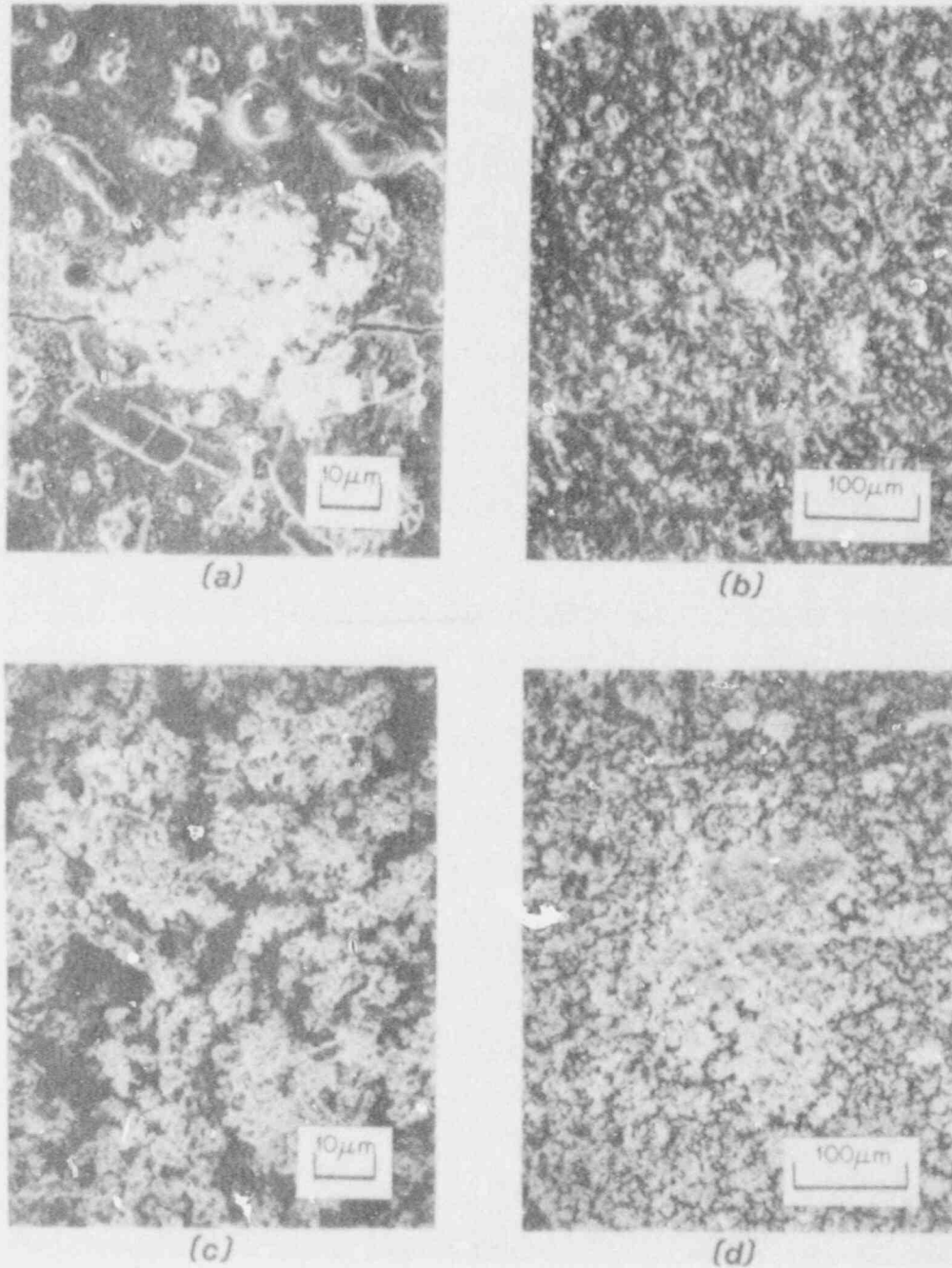


Fig. 8. SEM photomicrographs of surface deposits 8 cm, (a) and (b), and 16 cm, (c) and (d), into TGT B (test HS-2).

ORNL-PHOTO 330-86

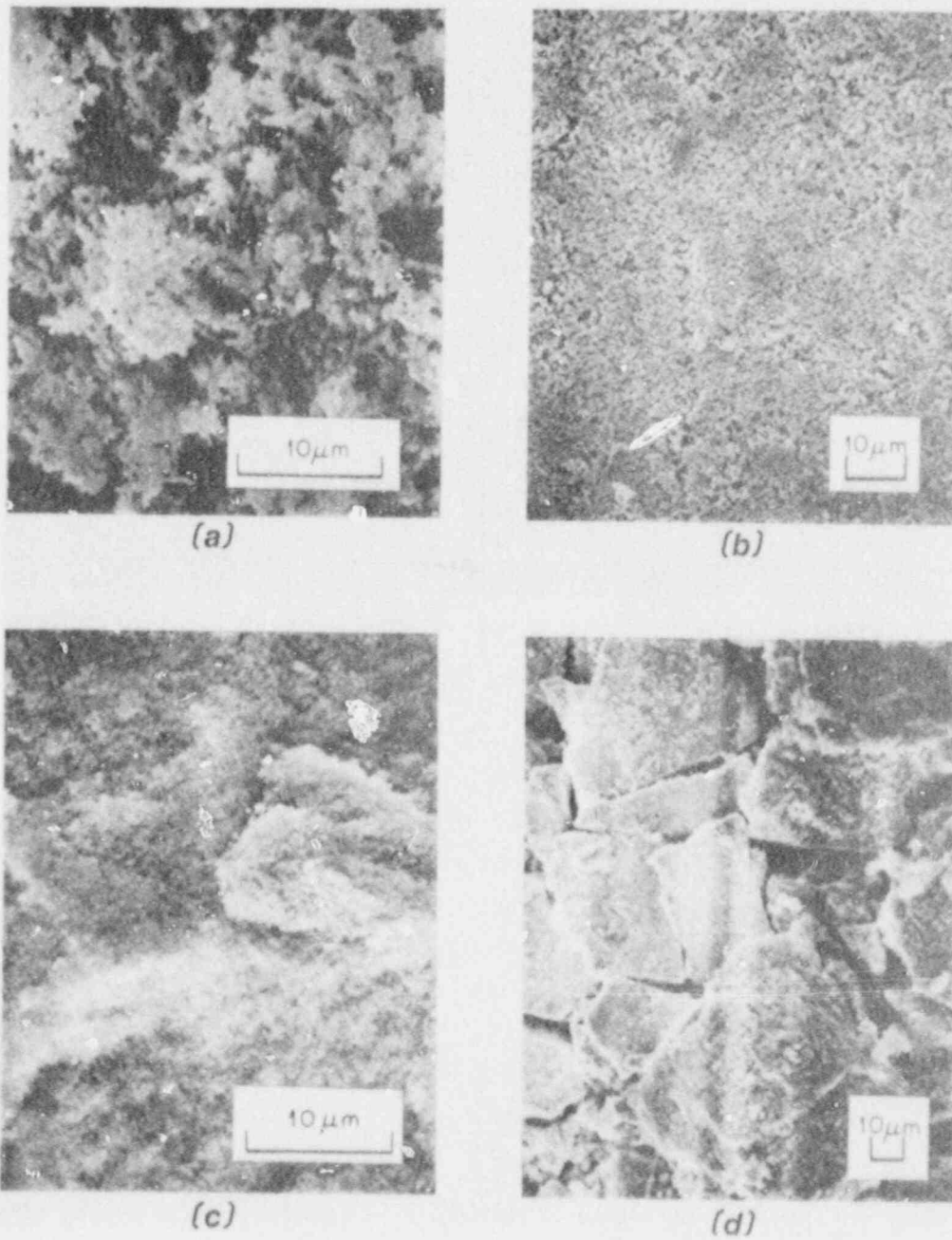


Fig. 9. SEM photomicrographs of surface deposits examined at 24 cm, (a) and (b), into TGT B (test HS-2). Aerosol deposit from the train "B" prefilter is shown in (c) and (d).

Table 3. Summary of relative X-ray intensities observed in various SEM/EDX samples^a

| Test and figure No. | Nominal relative peak height | | | | | | | | | | | | | | | |
|--|------------------------------|----|-----|-----|-----|----|----|----|-----|----|----|----|----|----|----|----|
| | Si | W | Pt | S | Ag | In | U | Cd | Sn | Te | Cs | Ba | Cr | Mn | Fe | Ni |
| <u>Test HS-2 (simulant fuel, 10 min at 2000°C plus 10 min at 2400°C)</u> | | | | | | | | | | | | | | | | |
| Fig. 5 (a) | | | 100 | | | | 33 | | 54 | | | | | | | |
| Fig. 6 (a) | 43 | | | | | | | | 100 | | | | | | | |
| Fig. 6 (c) | 18 | | | 15 | | | 15 | | 100 | | | | | | | |
| Fig. 6 (b) | | 18 | | | | | | | 100 | | | | | | | |
| Fig. 7 (b) | | 79 | | | | | 41 | | 100 | | | | | | | |
| Fig. 8 (c) | | 52 | | 19 | | | 30 | | 100 | | | 15 | | | | |
| Fig. 9 (c) | | 38 | | | | | 24 | | 100 | | | 14 | | | | |
| <u>Test HS-4 (simulant fuel, 5 min at 2000°C plus 15 min at 2450°C)</u> | | | | | | | | | | | | | | | | |
| Fig. 11 (a) | | 21 | | | 100 | | | | | | | | 12 | 13 | 12 | |
| Fig. 11 (c) | | | 100 | | 49 | 28 | | | | | | | | | | |
| Fig. 12 (b) | | 13 | | | 100 | | | | | | | | | 6 | 6 | |
| Fig. 12 (d) | | 15 | | | 100 | | | | 27 | | | | | 8 | 9 | |
| Fig. 13 (a) | | 16 | 100 | | | 13 | | | 26 | | | | | | 8 | |
| Fig. 13 (d) | | 19 | | | 100 | | | | 74 | | | | 18 | 14 | 79 | 19 |
| Fig. 14 (a) | | 19 | | | 100 | | | | 94 | | | | 13 | 11 | 45 | 15 |
| <u>Test VI-1 (irradiated fuel, 20 min at 1750°C plus 20 min at 2030°C)</u> | | | | | | | | | | | | | | | | |
| Fig. 16 (a) | 26 | | 100 | 65 | | | | | 47 | | | | | | | 19 |
| Fig. 16 (c) | | | | | | | | | 100 | | | | | | | 84 |
| Fig. 18 (a) | | | 54 | 100 | | | | | 65 | | | | | | | |
| Fig. 19 (a) | 100 | | | | | | | | 92 | 72 | | | 95 | | | |
| Fig. 19 (d) | 33 | | | 100 | | | | | 54 | | | | 34 | | | |
| Fig. 20 (b) | 38 | | | 100 | | | | | 48 | | | | 68 | | | |
| Fig. 20 (c) | | | | 100 | | | | | 60 | | | | 52 | | | |
| <u>Pretest VI-2 (no fuel, 10 min at 1725°C)</u> | | | | | | | | | | | | | | | | |
| Fig. 21 (d) | 100 | | 98 | | | | | | | | | | | | | |

^aApproximate values ($\pm 10\%$) normalized to maximum constituent.

5.2 HS-4 (SIMULANT FUEL HEATED TO 2000°C AND 2450°C)

5.2.1 Experimental Details

Much of the description of test HS-2 (Sect. 5.1.1) can be applied to test HS-4. The major differences between the tests were that in HS-4, a sample of Ag-In-Cd-Sn control rod alloy, clad in stainless steel and traced with ^{110m}Ag , and a stainless steel rod, traced with ^{51}Cr , ^{54}Mn , ^{59}Fe , and ^{60}Co , were laid alongside the simulant fuel specimen. Tin was included in the control rod alloy to simulate the composition of irradiated material. The heating cycle was similar to HS-2 except that phase A, at $\sim 2000^\circ\text{C}$, lasted only 5 min, while phase B, at $\sim 2450^\circ\text{C}$, was 15 min long. The gas flow was directed through TGT A until the temperature reached 2450°C ; TGT B received the gas flow throughout the remainder of the test, including cooldown.

Visual observation of the fuel specimen after the test showed extensive clad melting and oxidation. The thoria components had softened also, and there was substantial attack of the uranium pellets (Fig. 10). In the central region, the pellets had almost totally dissolved; severe attack had occurred to two-thirds of the pellets. Two foils of iridium metal (mp 2454°C) had been left in the thoria boat as melt indicators, one at each end. These were both located as droplets after the test, indicating that the melting point had been reached, and probably had been exceeded in the middle region of the specimen. No recognizable bulk remains of either the control rod or solid stainless steel rod could be found. There was extensive evidence of melting throughout the fuel rod area, and bright, metallic beads could be seen in the remains of the fuel.

As for HS-2, Zircaloy oxidation calculations for HS-4 were performed assuming (1) that no melting occurred and (2) a simple geometry-change melt model. The melting model shifted the period of steam starvation to a later time and extended it slightly. Both calculations showed full oxidation of all available Zircaloy shortly after the maximum temperature was reached. Clad melting had clearly occurred early in the test, and the interaction of liquid Zircaloy with uranium would tend to reduce the UO_2 and yield lower melting point alloys.⁶ Liquid stainless steel and control rod alloy may have accelerated this. These effects would tend to increase the time taken for full oxidation to occur and increase the time during which hydrogen levels remained high. Total material released from the furnace was measured at 2.269 g, about twice as much as in HS-2. Independent analyses confirmed that very little of the traced fission products, ruthenium and europium, were released from the furnace region, while substantial amounts of silver and manganese and smaller amounts of iron and chromium were released.⁴

5.2.2 Photomicrographs

Samples were taken from TGT A at 3 cm ($\sim 840^\circ\text{C}$), 16 cm (550°C), and 28 cm (280°C) and from TGT B at 2 cm ($\sim 810^\circ\text{C}$), 14 cm (590°C), and 32.5 cm (260°C). The TGTs have not been leached. Samples were also taken from

ORNL-PHOTO 7705-84



Fig. 10. Posttest view of the simulated fuel specimen used in test HS-4.

ORNL-PHOTO 321-86

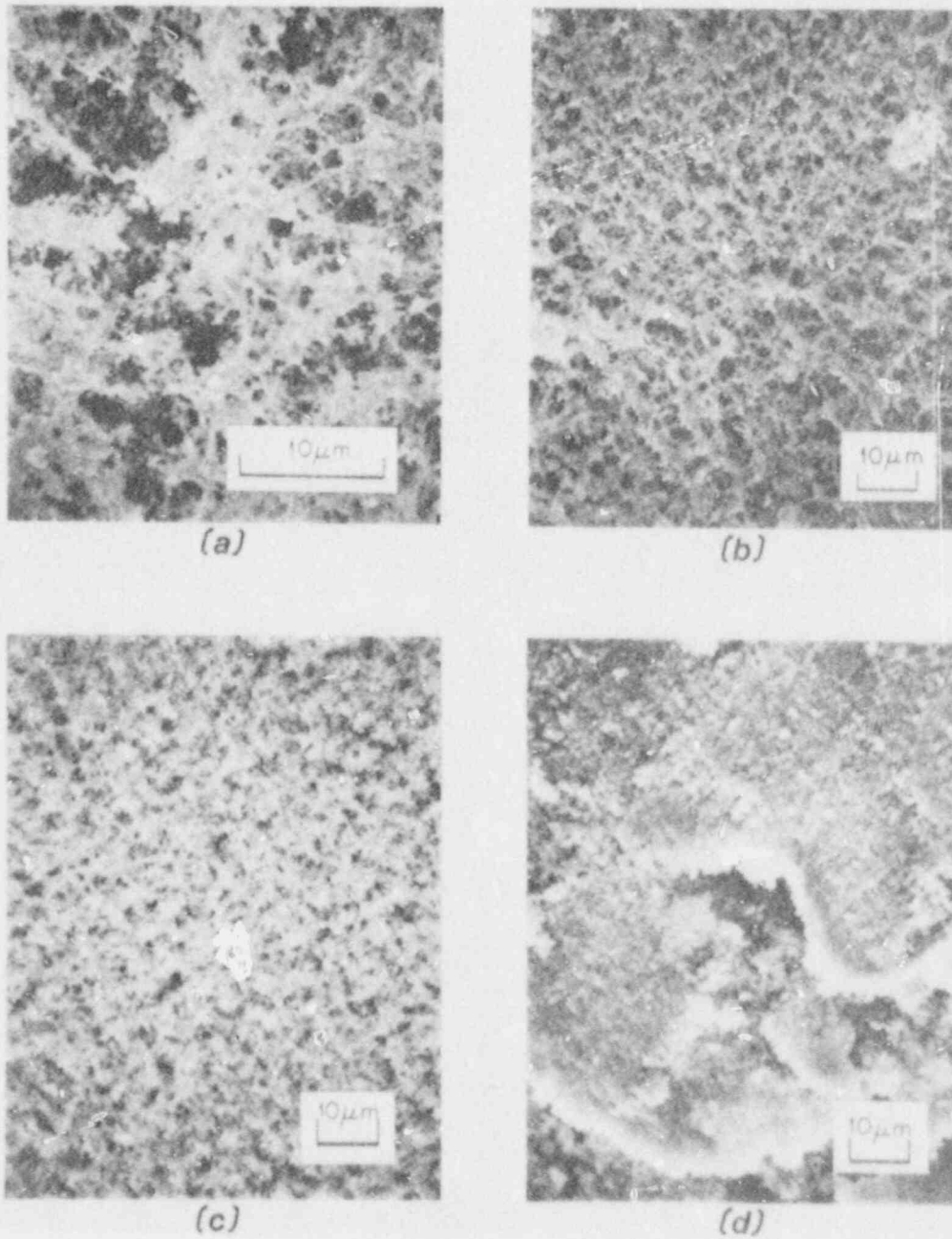


Fig. 11. SEM photomicrographs of surface deposits at 3 cm into TGT A (test HS-4).

the two glass wool prefilters ($\sim 150^\circ\text{C}$). Many of the analyses were dominated by silver, as the horizontal orientation of the experiment forced the control rod alloy to remain in the hot region of the furnace. The presence of cadmium meant that the separation of uranium and cadmium peaks in the EDX analysis was almost impossible (Table 2). The higher-energy X-ray lines from uranium (L-lines) could not be detected due to the low accelerating voltage of the instrument. Other elements detected were Sn, W (the thermocouple material), stainless steel components (Fe, Mn, Cr, and Ni), and In from the control rod alloy. At no stage did the fission products feature in the analysis; the ceramic contaminants did so only rarely.

The main features visible at 3 cm into TGT A, at 840°C (Fig. 11), were roughly spherical and consisted mostly of silver. Some of the larger "spheres" [Fig. 11 (a) and (b)] had many smaller "spheres" attached or coalesced with them. The sizes range from $\sim 50\ \mu\text{m}$ to $< 0.5\ \mu\text{m}$. Cadmium and indium may have been present, but the signals were not clearly separable from that of silver. Stainless steel components (Mn > Cr > Fe) were also detected in low concentrations in these analyses. The platinum surface could only be observed where the foil had overlapped on forming a tube. This showed considerable surface alteration [Fig. 11 (c) and (d)]. Some silver and indium were detected near this edge, possibly as an alloy with platinum. No tin was found in this region.

At 16 cm into TGT A, at 550°C [Fig. 12 (a) and (b)], silver featured very strongly again; however, the structures were quite different. The spheres were no longer in evidence and were replaced by small, angular, crystalline deposits ($\sim 1\ \mu\text{m}$) or a more porous, web-like or matted structure. The platinum signal was severely repressed; very little else was detected. This may be because the silver arrived after the first material (e.g., Sn) and covered it up. There appeared to be quite good adhesion of the deposits to each other and to the platinum surface but no evidence for or against a surface interaction.

The sample taken at 28 cm into TGT A (280°C) [Fig. 12 (c)] had rather loosely attached deposits. The silver signal was generally weaker, and cadmium dominated the response from the lower levels of the deposits. Where some of the original surface remained, the silver peak was higher again, indicating a time-dependent transport of these elements. The deposits were very fine ($< 0.5\ \mu\text{m}$) and quite porous. No stainless steel components were detected at this position.

The deposits on the filter were physically very similar to that which occurred in test HS-2, being a hard-packed mass of very fine particles ($< 0.1\ \mu\text{m}$), which broke easily into larger sheets [Fig. 12 (d)]. It was composed largely of Ag; some Sn and U were detected, and small amounts of stainless steel materials in the order Mn > Fe > Cr .

Samples from TGT B were not completely dominated by silver. The entrance region, at 2 cm (810°C) [Fig. 13 (a) and (b)], contained almost

ORNL-PHOTO 320-86

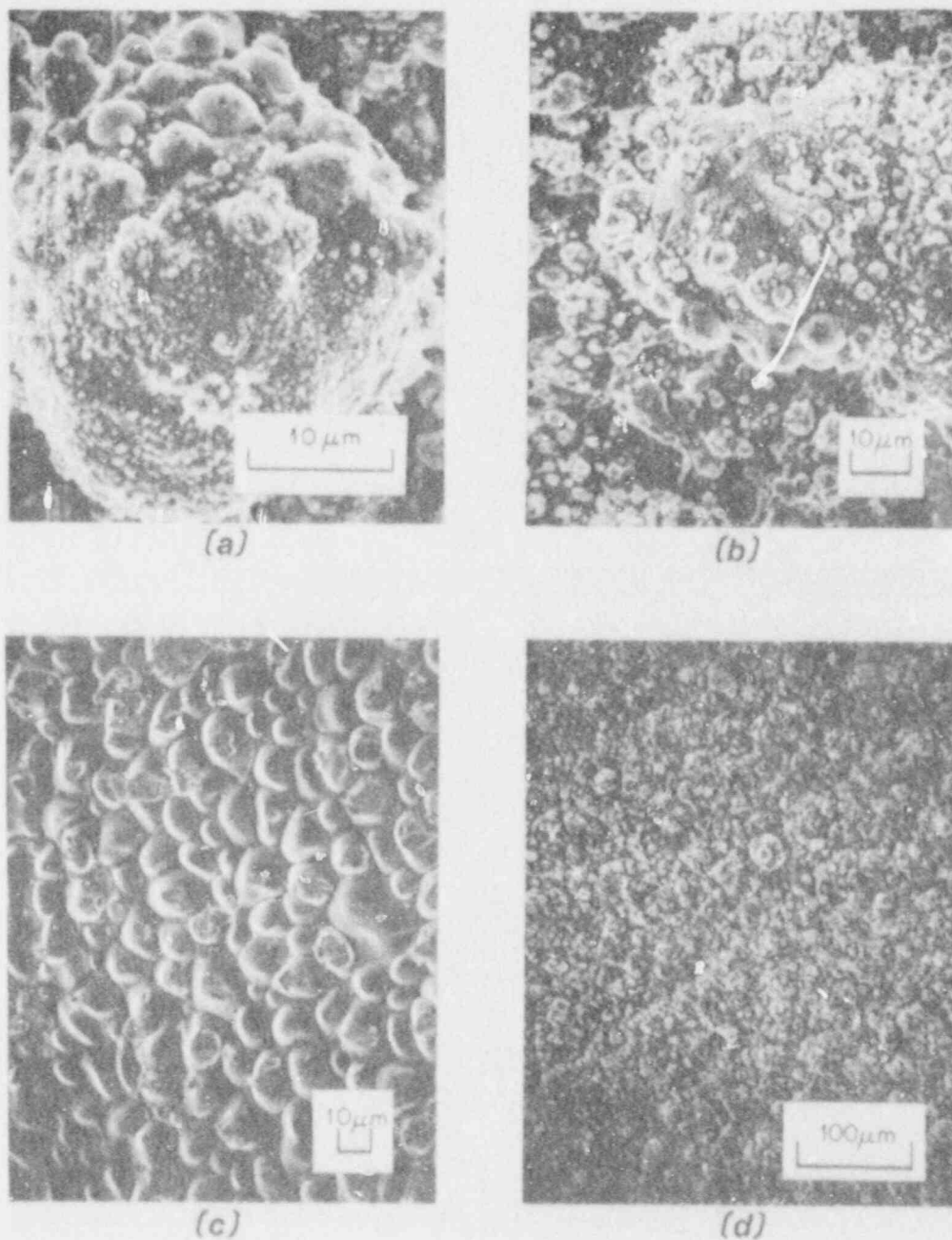


Fig. 12. SEM photomicrographs of surface deposits examined at 16 cm, (a) and (b), and 28 cm (c), into TGT A (test HS-4). Aerosol deposit from the train "A" prefilter is shown in (d).

ORNL-PHOTO 322-86

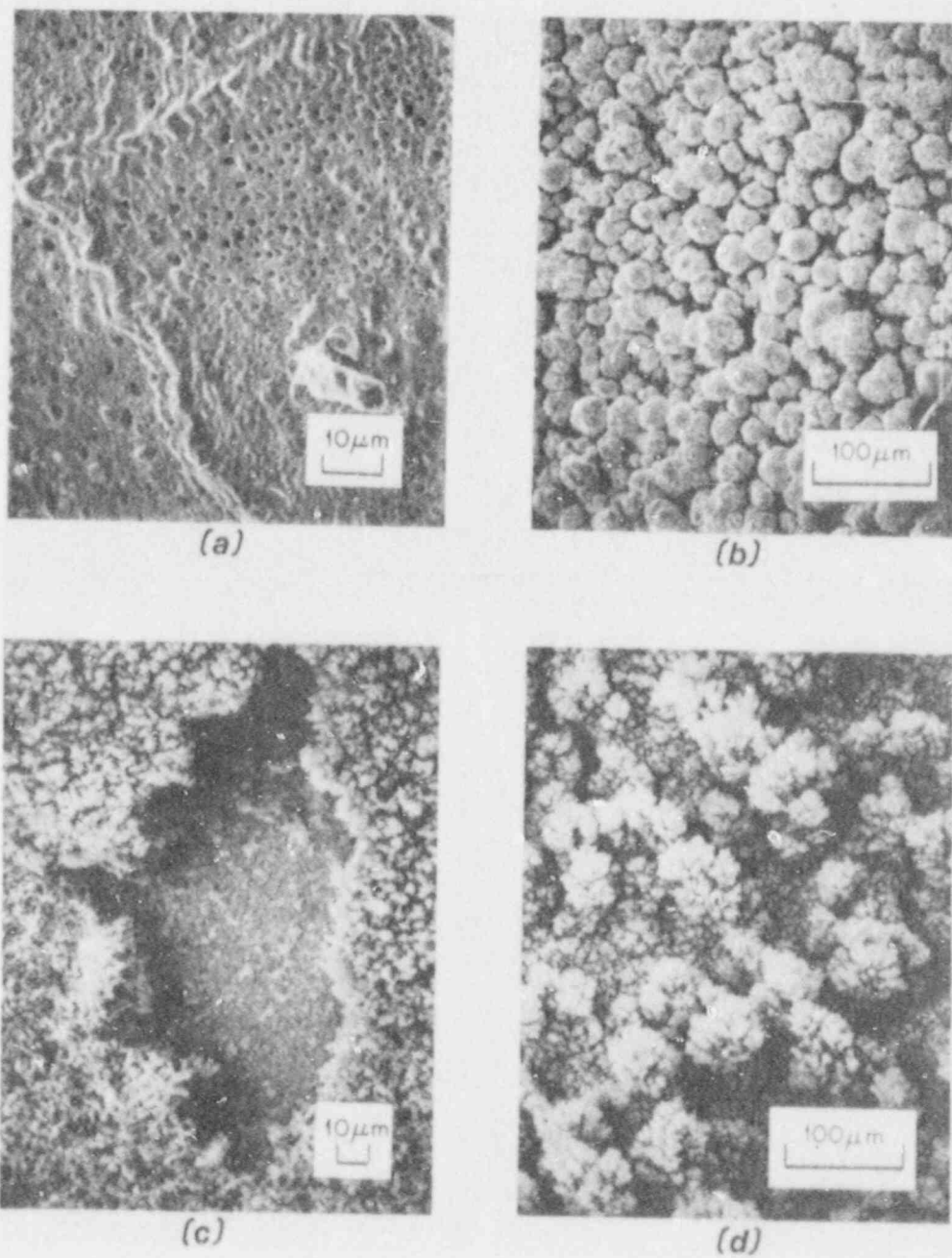


Fig. 13. SEM photomicrographs of surface deposits at 2 cm, (a) and (b), and 14 cm, (c) and (d), into TGT B (test HS-4).

no silver at all. The main signal was from platinum (8:1 over any other element), indicating very little deposition. However, the platinum surface was severely altered, with indication of grain boundary attack and grain eruption from the surface. A very porous structure resulted from these changes. Tin and indium were found associated with these features and may have promoted these effects by alloying. In some regions [e.g., Fig. 13 (a)], the surface appeared perforated by "bubbles," which could indicate incipient melting. The higher temperature in the furnace region would lead to a higher-than-expected surface temperature at this inlet region, maybe $>1000^{\circ}\text{C}$. A little Fe and S/Mo were detected in this region.

At 14 cm into TGT B, at 590°C [Fig. 13 (c) and (d)], silver again became important. The surface deposits were very thick, quite porous, and resembled coral growths. Tin and iron were the next most abundant elements. The deposits had quite good adhesion to each other but had flaked from the surface in large chunks. The surface itself appeared to be unaltered, but the lower deposits were richer in silver and relatively depleted in iron.

At 32.5 cm into TGT B, where the temperature was 260°C during test HS-4, the deposits showed a structure similar to all previous examinations in this temperature zone [Fig. 14 (a)]. A thick cake of small particles ($<0.5\ \mu\text{m}$), composed largely of silver and tin, was loosely adhering to the platinum substrate [Fig. 14 (a)]. Stainless steel elements were present in the following order: Fe $>$ Cr $>$ Mn $>$ Ni.

The aerosol deposits on the train B filter in test HS-4, which were composed largely of Ag, Sn, and Fe, consisted of very small ($<0.1\ \mu\text{m}$) particles bonded into thick sheets that broke from the mass quite readily [Fig. 14 (b)]. No uranium was identified in TGT B despite the severe attack of the fuel pellets in the furnace region. An SEM analysis of the bright beads in the partially dissolved uranium pellets shown in Fig. 10 demonstrated that they contained only ruthenium. They were in the approximate range 0.1 to 0.3 mm in diameter. None of the other added fission products had appeared to segregate in this way.

5.3 HI-6 (HIGH-BURNUP FUEL HEATED TO 2000°C)

5.3.1 Experimental Details

Test HI-6 is fully described in the data summary report issued in September 1985.¹ The fuel specimen used in this test was cut from a full-length rod that was irradiated in the Monticello BWR in Minnesota from May 1974 to February 1980, to a burnup of $\sim 40.3\ \text{Mwd/kg}$. The 15.2-cm-long section had cooled for $\sim 1400\ \text{d}$ when the experiment was conducted. Many short-lived isotopes had decayed away over this period, but longer-lived and stable isotopes of all important fission product elements remained in the fuel. The experiment was, in effect, a "transient" type. The test time was much shorter than planned due to a severe flow reduction shortly after the fuel reached the maximum temperature of $\sim 2000^{\circ}\text{C}$.

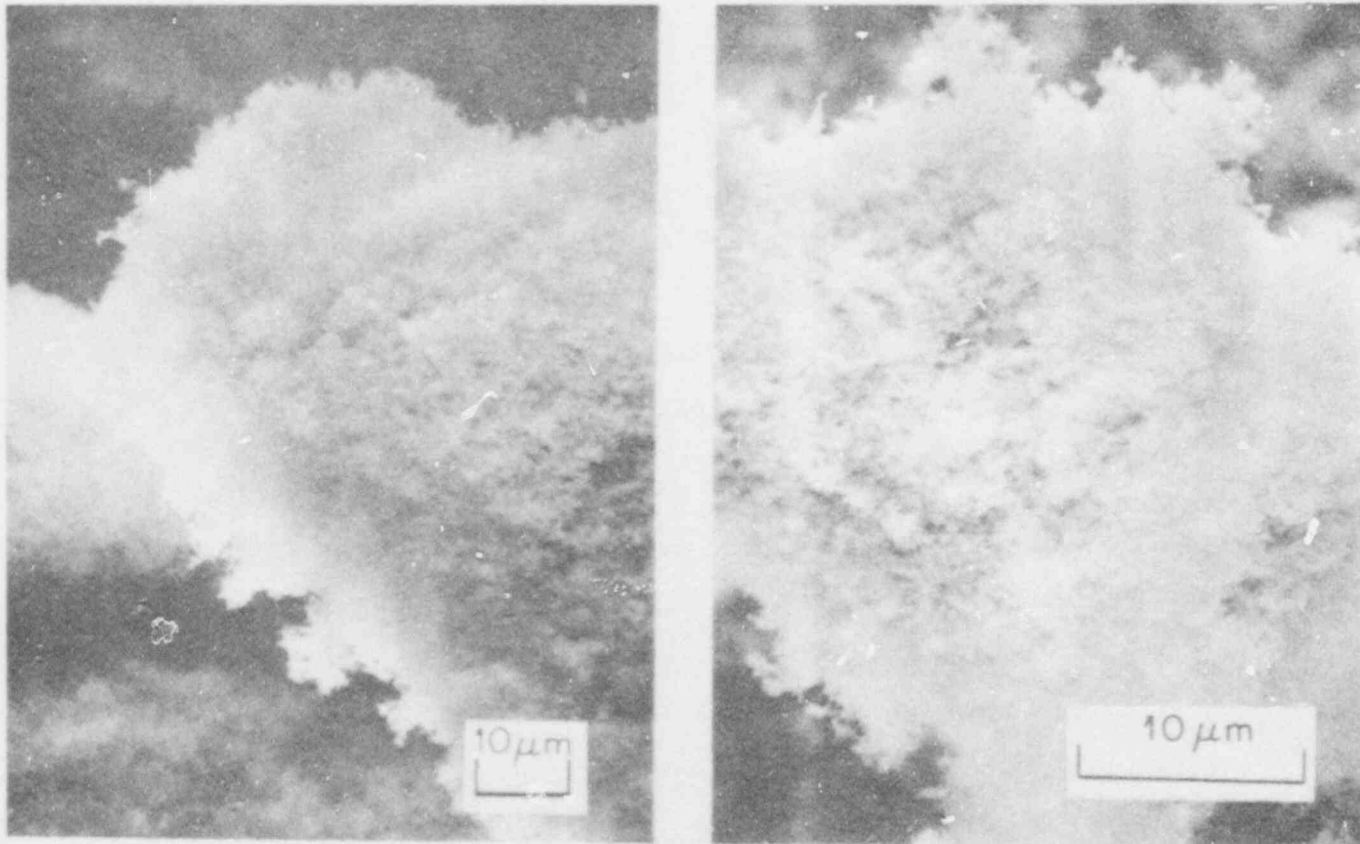


Fig. 14. SEM photomicrographs from test HS-4 of surface deposits at 32.5 cm, (a), into TGT B and of aerosol deposits from train B, (b).

This reduced the flow through the system to the extent that the experiment had to be terminated. The single, stainless steel TGT received the full system flow throughout the test.

Direct observation of the fuel was impossible, as it had become stuck to the zirconia furnace tube. It was cast in epoxy resin to retain orientation and cut radially for inspection. These sections showed heavy cladding oxidation at the inlet end and evidence of clad fracturing along most of its length. Very little oxidation had occurred near the outlet end, but some clad melting had occurred. These observations mean that steam starvation probably occurred at the outlet end for most of the time spent above 1100°C (24 min). A large crack in the cladding was observed in the radial sections to run for almost half the length of the fuel specimen. A total of 0.223 g of material was collected on the TGT and filters. Total releases from the fuel of 31.6% Kr, 33.1% Cs, and 24.7% I were measured. Sections of the TGT had been leached with a solution of simulated TMI-2 cooling water containing ~3750 ppm boron and ~1000 ppm sodium at a pH of 7.8 and $\text{NH}_4\text{OH}/\text{H}_2\text{O}_2$ followed by HNO_3 leaches. They were stored for ~2 years before examination by SEM.

5.3.2 Photomicrographs

The single TGT was sampled at 0-1 cm (~850°C), 16 cm (500°C), and 32 cm (250°C). The surface deposits had largely been dissolved away by the leaching process, and the micrographs show the exposed oxide structures on the stainless steel after the entire heating cycle and leaching. For comparison, an unheated sample of the same tube was also examined before and after leaching with the same chemicals ($\text{NH}_4\text{OH}/\text{H}_2\text{O}_2$ followed by HNO_3/HF).

The inlet region at 0 cm [Fig. 15 (a)] showed needle-shaped oxide growth overlying an area where grain boundaries have been emphasized or etched. Needles of this type are generally indicative of early-stage oxidation. Moving along the 1-cm-long piece of steel, the needles rapidly disappeared, to be replaced by exposed grain surfaces, deeply pock-marked with severe attack at the grain boundaries [Fig. 15 (b)]. Several particles, some spherical, were seen on these exposed surfaces. These particles were probably not part of the original surface deposits.

In the next region examined, at 16-18 cm, at 500°C (Fig. 16), pock-marked grains and grain boundary attack can again be seen [Fig. 16 (a) and (b)]. The degree of attack was less than encountered at 0-1 cm. These grains are beneath a thick layer of oxide that appeared to be poorly attached to the exposed grains. This oxide layer was composed of rounded lumps with no appearance of crystallinity.

At the outlet end (250°C), a much smoother oxide surface could be seen [Fig. 16 (c)], in which the cracks do not necessarily relate to grain boundaries. Some areas in which the continuity of the oxide had been broken were observed. Only limited evidence of grain boundary attack or pitting appeared in these areas. The only elements detected in

ORNL-PHOTO 332-86

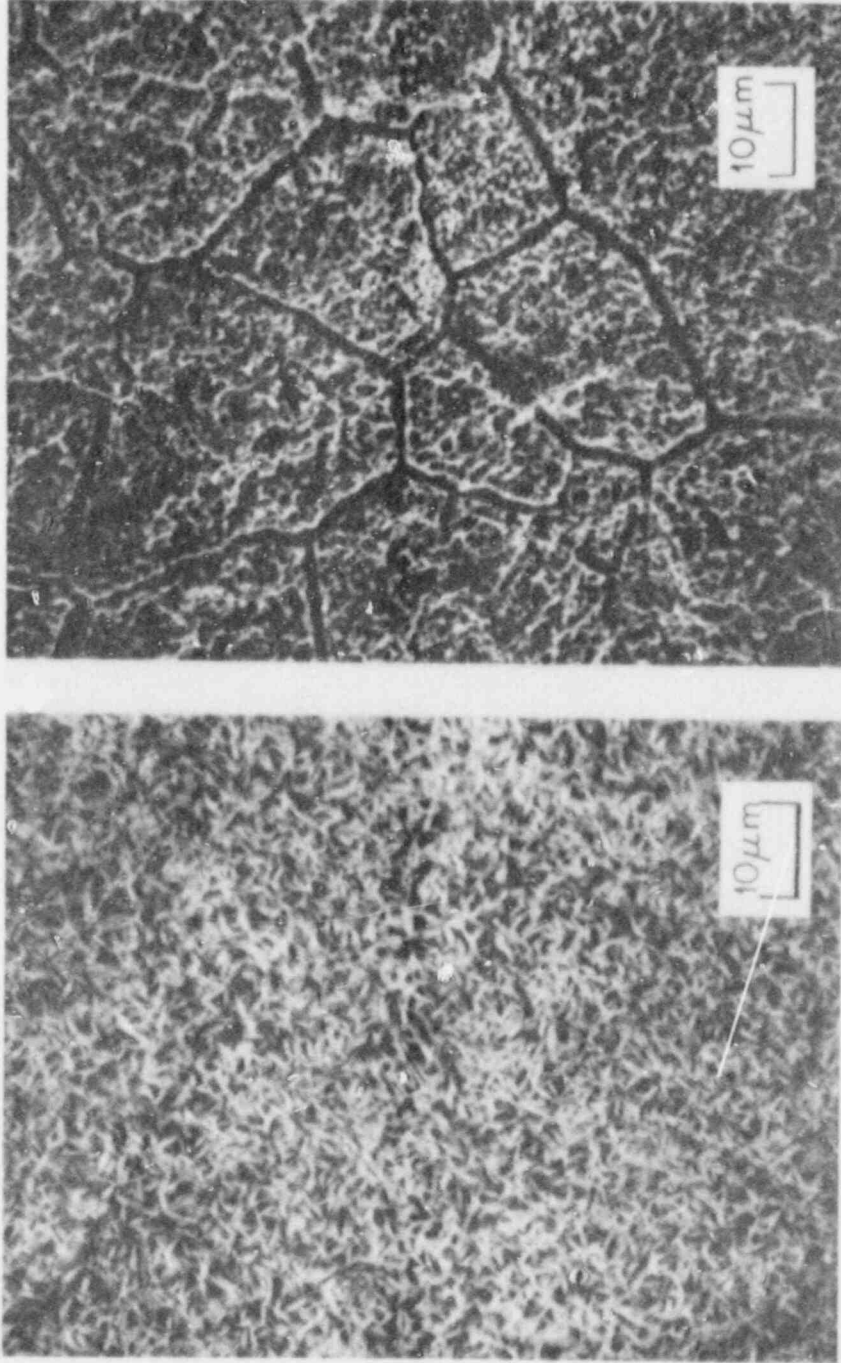


Fig. 15. SEM photomicrographs of deposits from the entrance region, (a), and ~1 cm, (b), into the TGT (test HI-6).

ORNL-PHOTO 324-86

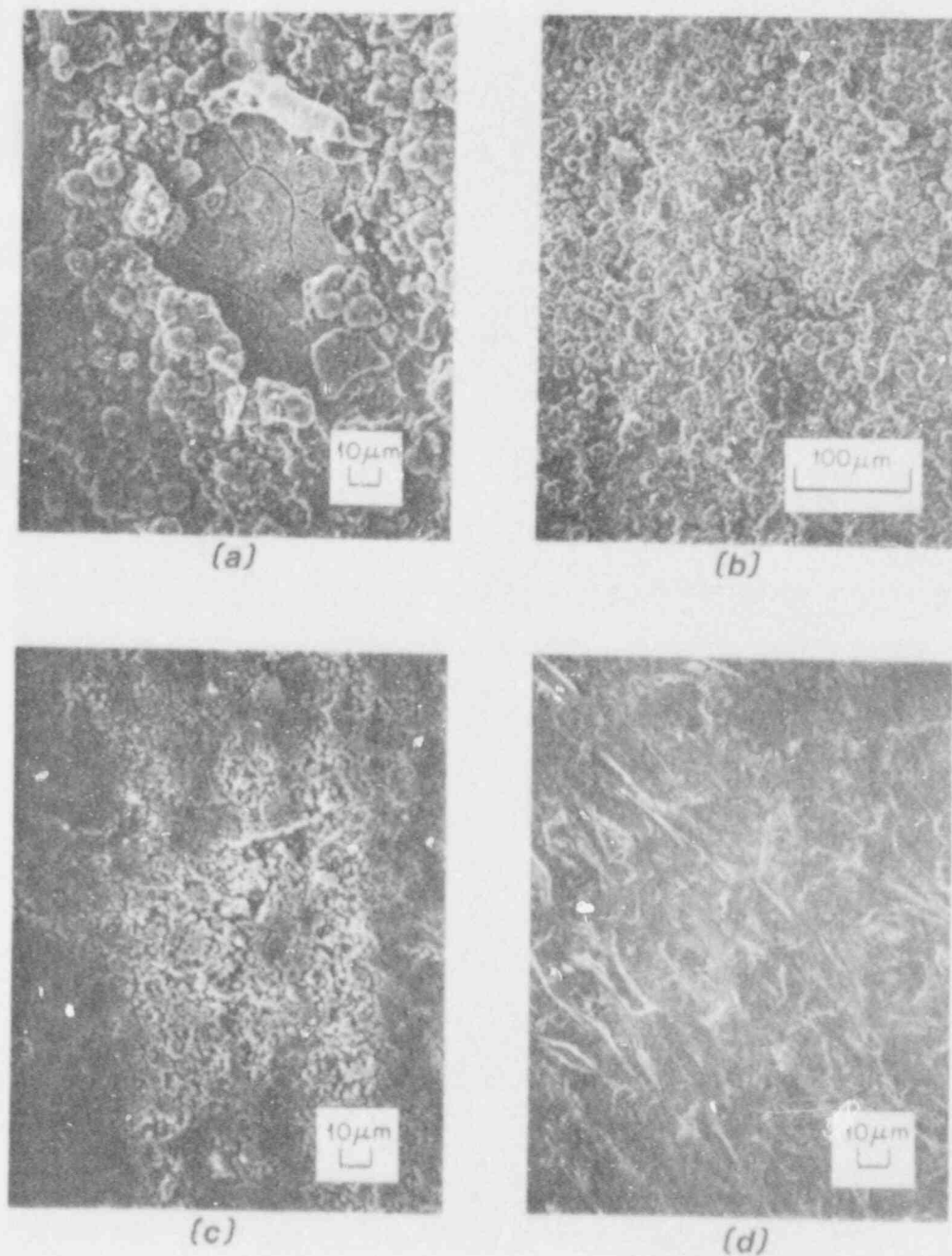


Fig. 16. SEM photomicrographs of surface deposits examined at 16 to 18 cm, (a) and (b), 32 cm, (c), and of an unheated but leached material (test HI-6).

any of these analyses were Fe, Cr, Ni, and Si. Activity levels remained quite high at the central region (16 to 18 cm); this may be due to cesium retention in the oxide structure.

The archive sections of tubing that had not been heated did not show any grain boundary attack or pitting, even after the leaching cycle (4 h in $\text{NH}_4\text{OH}/\text{H}_2\text{O}_2$; 2 h in HNO_3/HF) [Fig. 16 (d)]. The surfaces were not smooth, and occasionally grain outlines or missing grains could be observed. The general impression given by the unheated surfaces was of a smearing out of the surface structure, which is probably a consequence of the forming processes. As a followup to these studies, metallographic samples of the tube at 0 cm, 1 cm, and 32 cm and of the unheated, but leached samples were prepared and examined. Very little difference was found among any of these samples. A slight roughening of the surface was observed at the inlet regions (0 and 1 cm), but no evidence of deep grain boundary etching or growth/alteration could be detected. It appears that for the short time at the temperatures experienced in this test, only surface attack occurred.

5.4 VI-1 (HIGH-BURNUP FUEL HEATED TO 1750°C AND 2030°C)

5.4.1 Experimental Details

Test VI-1 was the first test using commercial fuel to be conducted in the vertical orientation.⁷ The furnace concept was similar to that used in the horizontal tests, although several design changes had been made.⁸ The fuel specimen was cut from a full-length rod that was irradiated, in the Oconee PWR in South Carolina from February 1975 to November 1979, to a burnup of ~42 MWd/kg. The 15.2-cm-long section had decayed for ~2200 d when the experiment was conducted; short-lived isotopes had decayed away, but all the elements of interest were present. The three TGTs were used to monitor three phases of the test; TGT A received the flow from heatup to the end of the stable period at 1750°C, TGT B received the flow during the ramp to 2030°C and for 5 min at that temperature, and TGT C received the flow for the remaining 15 min at 2030°C and the entire cooldown period. Direct observation of the fuel was not attempted after the test. The fuel orientation was preserved by casting the specimen in epoxy resin and cutting it radially to examine for cracking and cladding oxidation. All sections showed extensive oxidation, and several openings in the zirconia clad were observed. There was little evidence of clad melting or clad/fuel interaction. Calculations of steam oxidation were performed that showed essentially complete oxidation of the original Zircaloy cladding shortly after the fuel temperature reached 1700°C.⁵ Further hydrogen was produced throughout the test from oxidation of the thicker Zircaloy end caps and the graphite-steam reaction caused by leakage of steam into the susceptor region of the furnace. Estimates of leakage are that up to 30% of the total flow passed through this region. Thus, the hydrogen level was maintained at ~30% of its maximum through most of the test. Total releases from the fuel of 57% krypton and 74% cesium were measured. A total of 1.08 g of material was collected on the three TGTs and filters. Samples of TGT were cut before

leaching; the regions of choice were based on concentrations of ^{137}Cs observed during the gamma-scanning of the tubes.

5.4.2 Photomicrographs

Samples were cut from the three TGTs as follows: TGT A, 1 cm ($\sim 860^\circ\text{C}$), 11 cm (600°C), 16 cm (520°C); TGT B, 1 cm ($\sim 860^\circ\text{C}$), 34 cm ($\sim 200^\circ\text{C}$); TGT C, 1 cm ($\sim 880^\circ\text{C}$), 6 cm (730°C), 15 cm (550°C).

Samples were also taken from the glass wool prefilters of trains B and C, which were heated to $\sim 150^\circ\text{C}$. The elemental analysis of the deposits in the TGTs was complicated by the presence of impurities from the ceramics, especially S, Si, and to a lesser extent, Ca. However, Sn, Cs, Te, U, and Mo were unambiguously identified at various positions in the TGTs. Data from spark-source mass spectrometry and neutron-activation analysis were used in conjunction with the SEM data to clarify issues, where possible.

The inlet end of TGT A, where there was a temperature of 860°C [Fig. 17 (a) and (b)], showed a range of structures and fairly thin deposits. The surface was cracked, due to the embrittlement of the tube by the deposits. The platinum signal was strong, and variable amounts of Sn, Cs, S, and Si were also detected. The log-like structures consisted mostly of platinum, while the whiskers were largely sulfur. The uneven surface contained more tin than the other features; cesium appeared to be spread fairly evenly over the surface.

At 11 cm into TGT A (600°C) [Figs. 17 (c) and 18 (a)], selected because of a peak in the cesium profile, discrete piles of cubic crystals were observed. X-ray analysis indicated the presence of cesium only; these crystals may have been deposited as CsOH liquid that solidified on cooling to form the crystals. The hygroscopic nature of CsOH prohibits much interpretation of the size and shape of the crystals after exposure to moist air, but they varied between ~ 2 and $12\ \mu\text{m}$ across. The only other element detected was tin; the deposits were very thin, and some interaction with the platinum was observed at grain boundaries, possibly a Pt/Sn alloying. A further sample from this region was examined after leaching in basic and acidic leaches [Figs. 17 (d) and 18 (b)]. The crystals were gone, leaving a faint residue and some evidence of Pt/Sn interaction.

At 16 cm into TGT A, at a temperature of 520°C [Fig. 18 (c) and (d)], a similar appearance was observed. The deposits were thin, and discrete clumps of cubic cesium-containing crystals were evident. Tin formed the remainder of the deposit. Some evidence of tellurium was obtained from one analysis, but the SSMS sample did not confirm this.

The sample from the inlet region of TGT B (860°C) [Fig. 19 (a), (b), and (c)] showed some very different structures. A large range of features was observed, from spheres to thick whiskers. The furnace temperature was raised during this portion of the test, and considerably more sulfur

ORNL-PHOTO 325-86

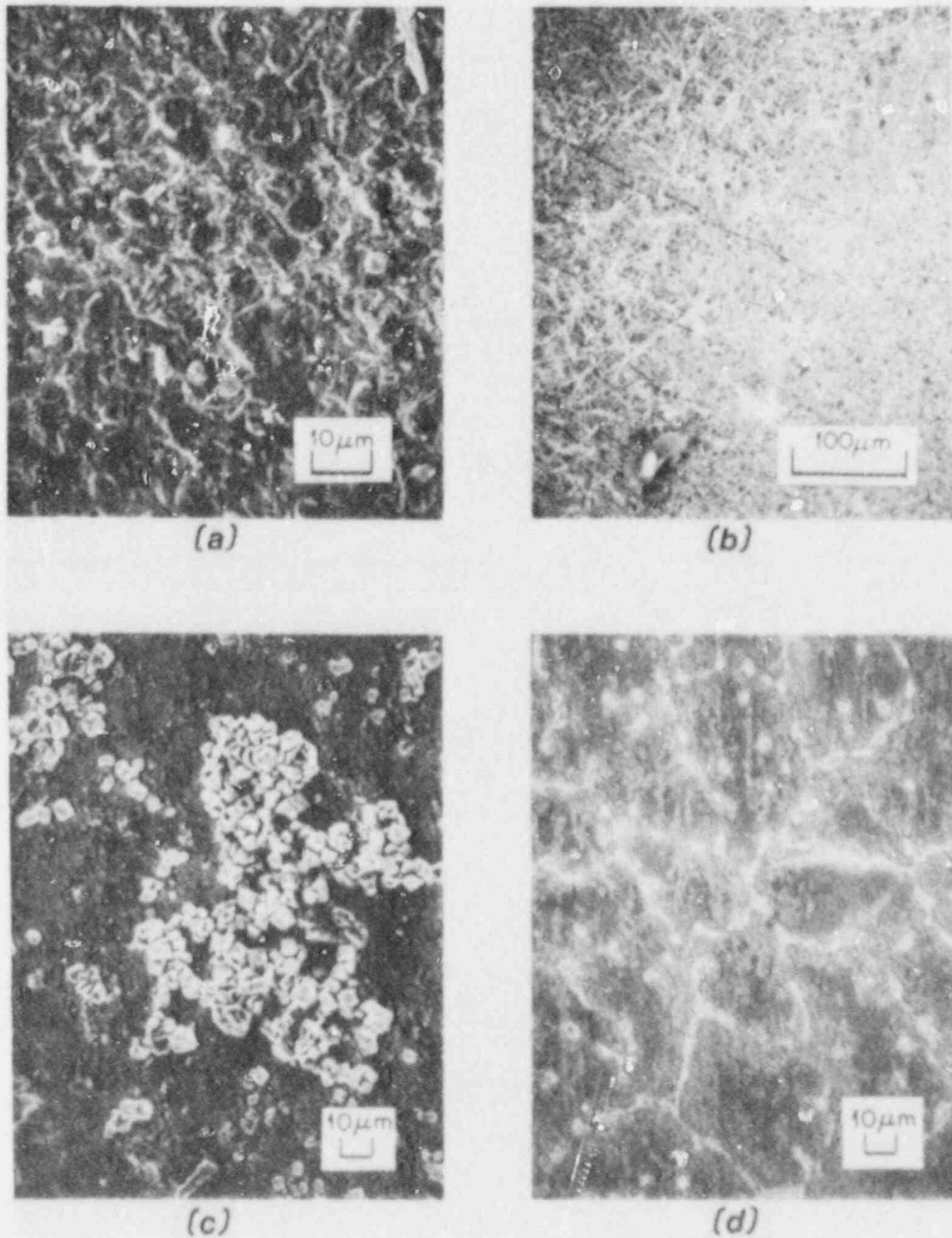


Fig 17. SEM photomicrographs of surface deposits at the inlet end, (a) and (b), and 11 cm, (c), into TGT A (test VI-1). The view in (d) shows the surface at 11 cm after it was leached in basic and acidic leaches.

ORNL-PHOTO 326-86

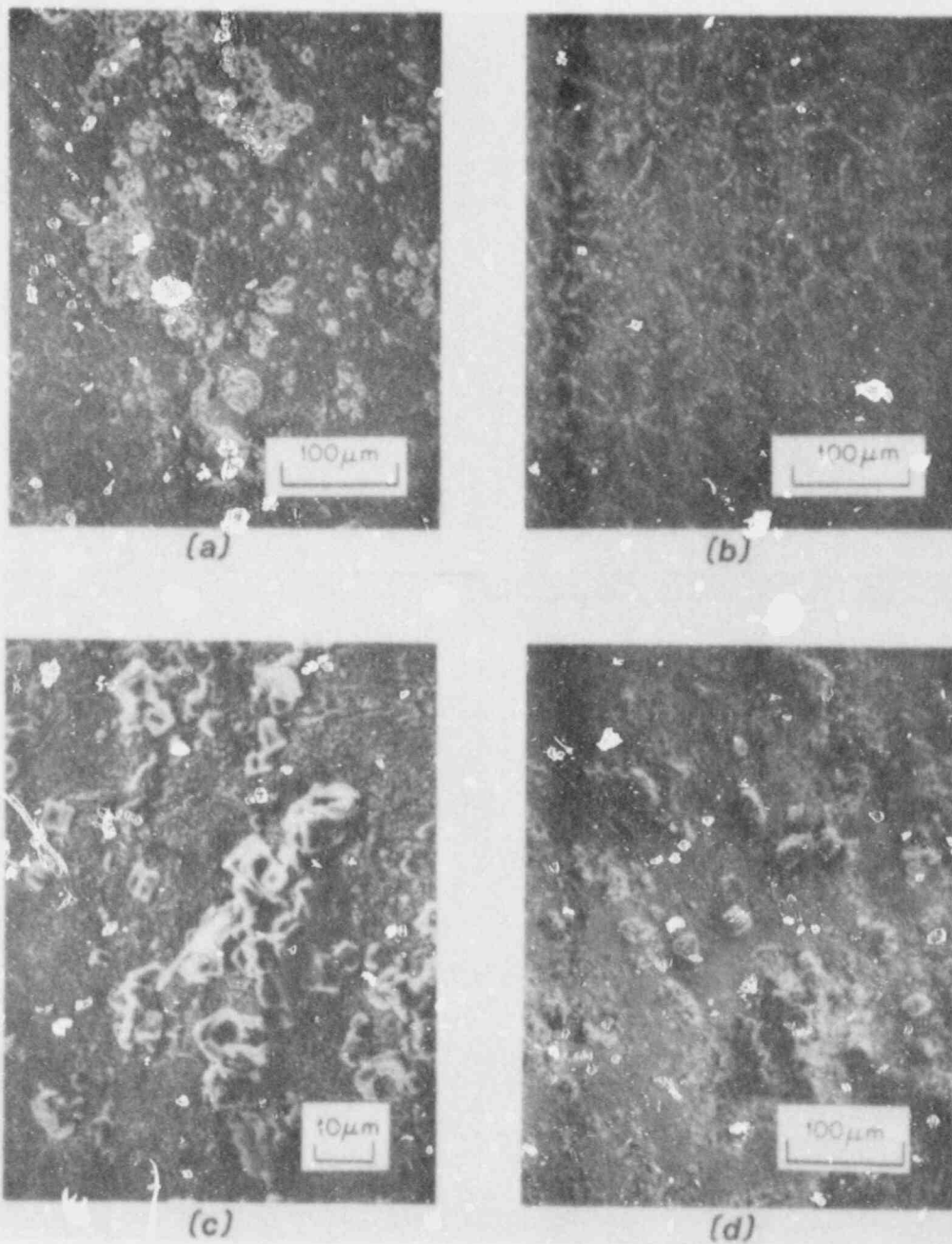


Fig. 18. SEM photomicrographs of surface deposits at 11 cm, (a), and 16 cm, (c) and (d), into 2GT A (test VI-1). The view in (b) shows the surface at 11 cm after it has been leached in basic and acidic leaches.

ORNL-PHOTO 327-86

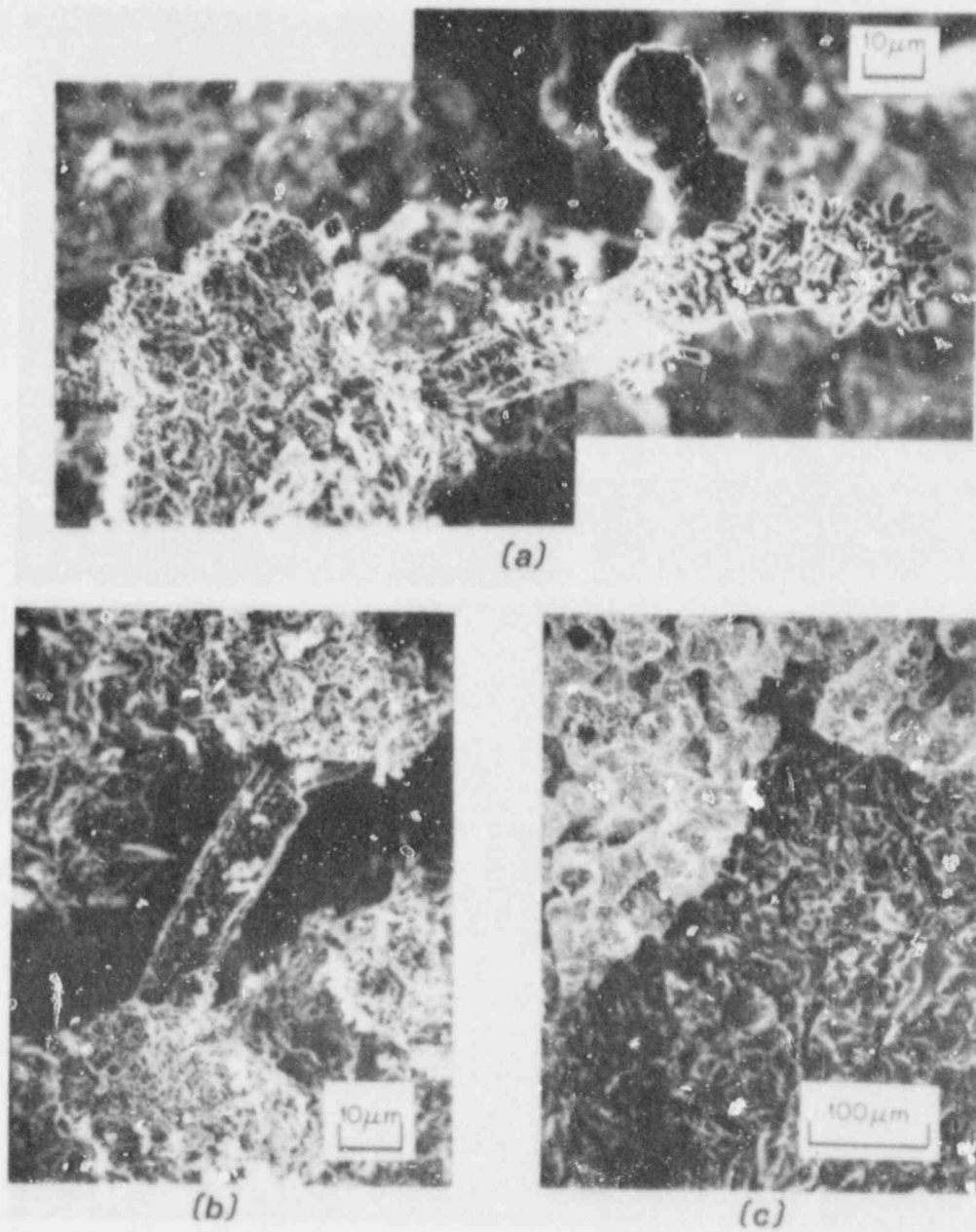


Fig. 19. SEM photomicrographs of surface deposits at the inlet region of TCT B (test VI-1).

and silicon were detected among the deposits. The deposits were not very thick, as platinum was always strongly featured in the X-ray spectrum, but the surface had become extremely porous with some complex interactions occurring. The general appearance was not unlike that of the inlet region of TGT B in test HS-4 (Fig. 13). Where the reacted surface had flaked away, the platinum beneath was severely altered but did not contain a measurable amount of impurity. Platinum strands appeared to have erupted from grains and then reacted with sulfur and silicon to form crystallite side growths on the strands. The spherical objects [Fig. 19 (a)] may have been enriched in cesium. Some tungsten was also observed, presumably from the thermocouple material. A further sample from this region was examined after basic and acidic leaches. No pictures of this region are shown, but little difference was visible; some rounding of edges was observed, but the large structures had not been leached from the surface.

The outlet end of TGT B (200°C) (Fig. 20) was the only sample from a cool region of a TGT from test VI-1 that was examined. This was because the poor deposit-to-surface adhesion gave contamination problems in the SEM sample chamber. Gold coating of future samples would probably help to prevent the flaking and dispersion of this fine material. Very fine particles (<1 μm) were observed in the deposit, containing a few small rounded particles (~3 μm) trapped in the matrix. The platinum signal was repressed in some cases, indicating a thick deposit. High levels of Cs, Sn, and Te were recorded. The SSMS data confirmed the presence of tellurium in this region. Silicon and sulfur were also present in moderate amounts.

The material on the train B filter was predominately tin. However, small quantities of uranium were also detected (the fuel sample contained little cadmium). Small amounts of cesium were present, and a response in the P/Zr/Pt area was found. The particles appeared to be uniformly small (<0.1 μm) and packed tightly into cakes that broke up into flat sheets quite readily. No photographs from this filter are shown.

Deposits on samples from TGT C were released while the fuel was at 2030°C and during the cooldown period. The inlet region (880°C) [Fig. 20 (c) and (d)] showed none of the heavily matted and grossly disrupted surface structures that were seen in TGT B. The platinum surface was visible over much of the sample and gave a high response on the X-ray spectrum. Tin was heavily represented in most areas along with cesium and the contaminants sulfur and silicon. Particles of ~2 to 5 μm were found over most of the surface. Some evidence for platinum grain boundary attack was observed.

At 6 cm into TGT C (730°C) [Fig. 21 (a) and (b)], the matted surface was seen again. The deposits were heavy (platinum signal was repressed), and a great deal of cesium was found, along with substantial amounts of sulfur; rather less tin and silicon were located than before. Whiskers similar to those at the inlet region of TGT B, although not as heavily reacted, were also observed. It was not possible to positively identify cesium-rich particles.

ORNL-PHOTO 328-86

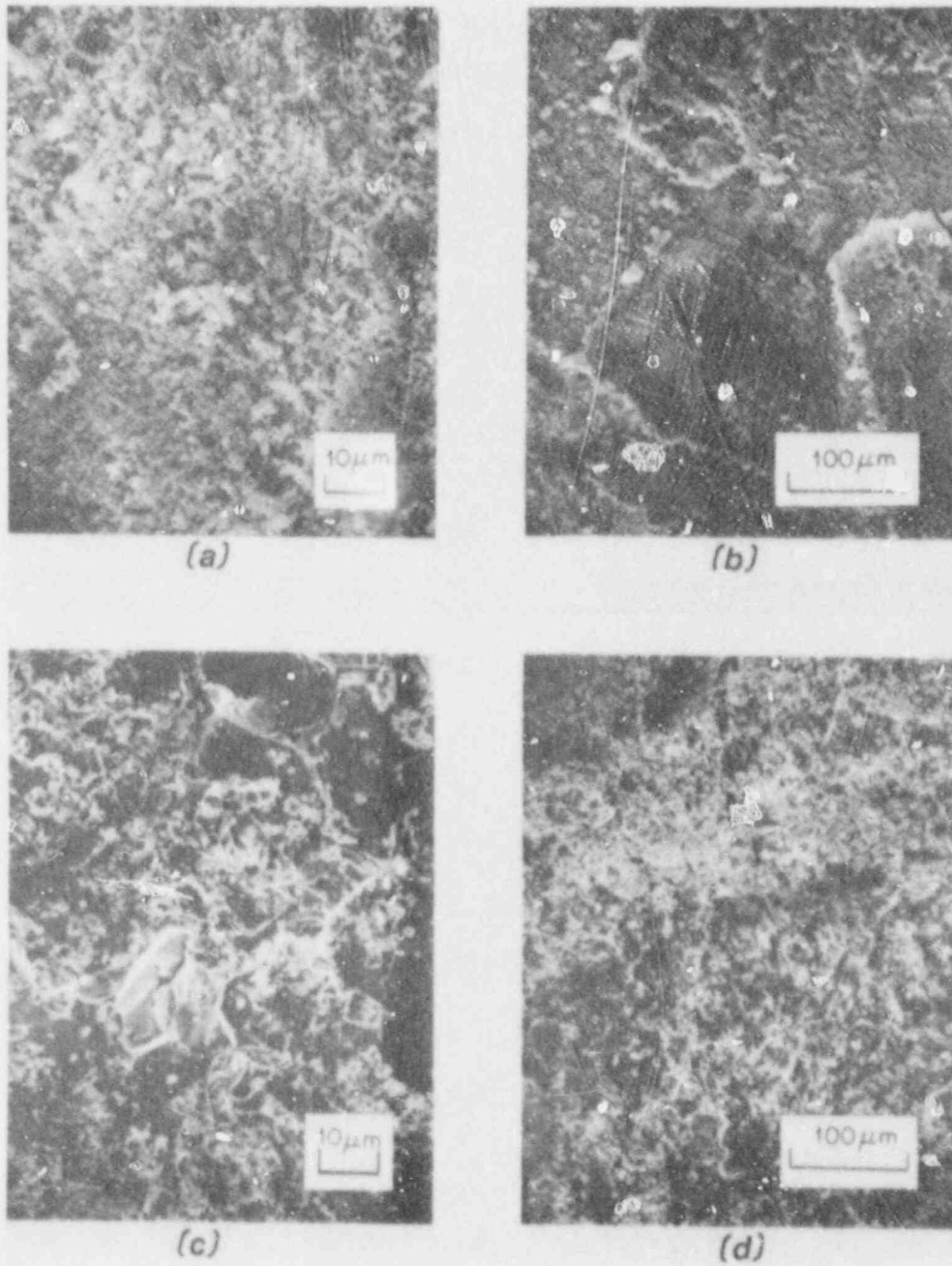
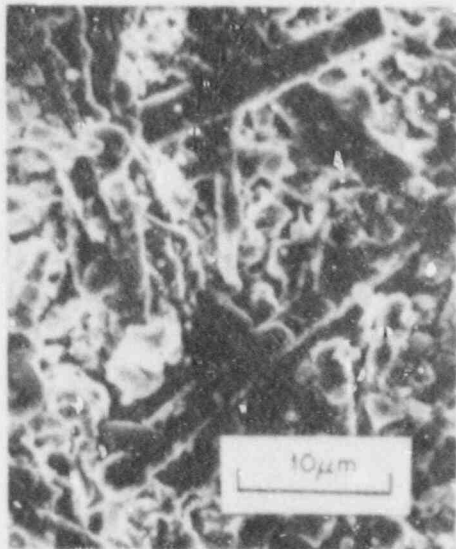


Fig. 20. SEM photomicrographs of surface deposits examined at the outlet end, (a) and (b), of TGT B and the inlet end, (c) and (d), of TGT C (test VI-1).

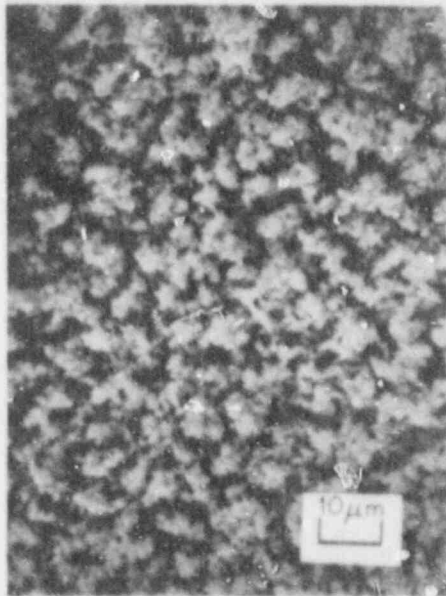
ORNL-PHOTO 329-86



(a)



(b)



(c)



(d)

Fig. 21. SEM photomicrographs of surface deposits at 6 cm, (a) and (b), and 15 cm, (c), into TGT C (test VI-1). The view in (d) shows the surface at 15 cm after it was leached in basic and acidic leaches.

At 15 cm into TGT C (550°C) [Fig. 21 (c)], heavy, porous, coral-like deposits containing Cs, S, and Sn were found. The platinum signal was severely repressed. The deposits were very uniform and were observed to lift off in chunks. Analysis beneath these areas showed higher levels of tin. Several reacted "whiskers" were found lying on top of the main deposits.

A further sample from this region was examined after basic and acidic leaches [Fig. 21 (d)]. The porous deposits had largely disappeared from the surface, leaving a smoother and finer surface which was predominantly tin.

The aerosol deposits on the filter beyond TGT C were mostly of tin, with measurable amounts of Cs, S, and Si and a hint of uranium. The physical appearance was similar to all other filter deposits, being a very fine, tightly packed deposit. No photographs are shown.

5.5 VI-2 PRETEST (FURNACE HEATED TO 1725°C)

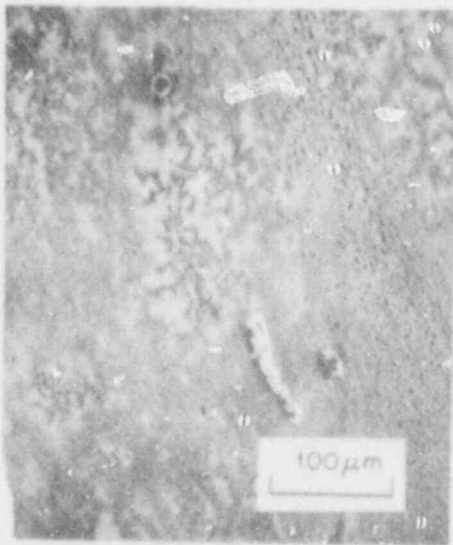
5.5.1 Experimental Details

Prior to conducting the full-scale hot test, VI-2, a pretest was run to check the furnace operation and temperature measurement. A single TGT and filter were placed above the furnace, and the temperature was raised to 1725°C for ~10 min. There was no fuel rod in the furnace region, and only the material released from the ceramics would be expected in the TGT. This test may be most closely compared to the TGT A portion of test VI-1, without the fuel present. The TGT gained 7 mg in weight; visual inspection showed that deposits were thick enough to dull the metal near the inlet end but not near the outlet end.

5.5.2 Photomicrographs

Samples were cut from the TGT at 1, 6, 15, and 36 cm. Deposits were quite light in all regions except at the outlet end where a slight discontinuity in the smoothness of the platinum foil appeared to have trapped a small pile of particles. These resembled the platinum-rich whiskers seen in TGTs B and C of VI-1. They were also present on the prefilter surface, and contained varying amounts of silicon and platinum with little evidence for the presence of sulfur. Deposits at 1, 6, and 15 cm into the TGT had a similar appearance [Fig. 22 (a), (b), and (c)], with the density of the deposits being the major difference. Some spherical particles (5-20 μm) composed mainly of calcium were located as well as smaller irregular lumps containing mostly silica. These often appeared to be at the center of a reacted area of the surface [Fig. 22 (b)]. A zone of surface disruption surrounded these particles with "reaction fronts" extending up to 0.2 mm from the center. A few platinum-containing whiskers were located in these regions. The platinum surface appeared to have become porous in the reaction zones; adjacent regions had not been affected. Some sulfur was located at the 15-cm location.

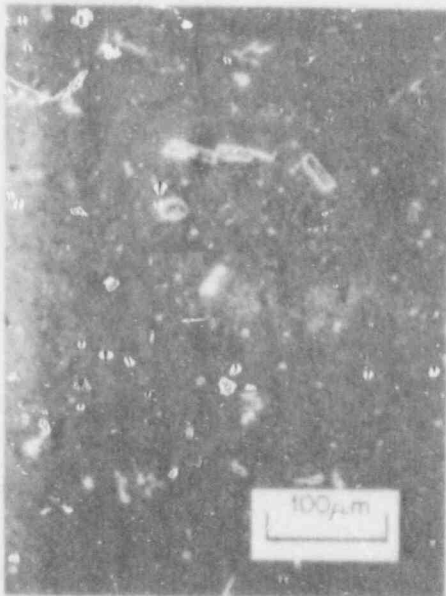
ORNL-PHOTO 331-86



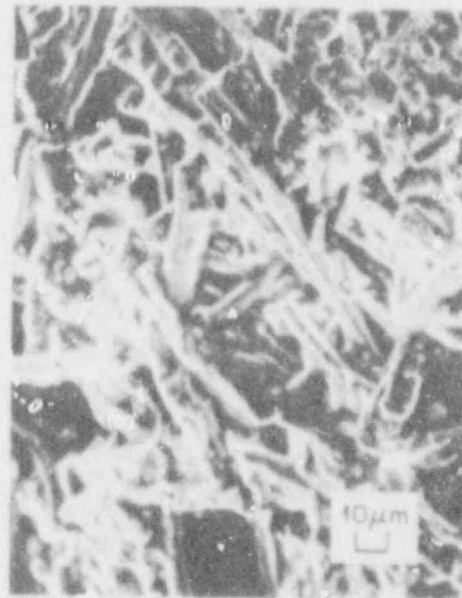
(a)



(b)



(c)



(d)

Fig. 22. SEM photomicrographs of surface deposits at 1 cm, (a), 6 cm, (b), 15 cm, (c), and 36 cm, (d), into the TGT used in pretest VI-2.

6. DISCUSSION

In any series of experiments seeking to model a large and complex system in a smaller and simplified arrangement, there will be shortcomings. The necessity of using a small, electrically powered furnace in the present work rather than large-scale nuclear heating has led to the introduction of materials that are not usually present in the primary coolant system of a nuclear reactor (e.g., S, Ca, Si). Platinum has been used as an "inert" surface for the collection of volatilized species from the fuel, but it has been affected by some of these materials. This has led to a changed, more reactive surface in some cases. The failure of platinum TGTs to behave in a "model" way on an intermittent basis in the past may be partly due to these factors. Despite this, it is likely that stainless steel tubes, although providing a much more realistic surface in a reactor context, would have suffered even more severe alteration from the furnace contaminants. It is probably important to use stainless steel TGTs in some future tests, but it must be emphasized that release of contaminants from the furnace region must be minimized if representative behavior is to be observed. However, information gathered in this study will be useful in the design and interpretation of future experiments.

Surface examination by an SEM can cover only a small fraction of such a large area, such as a thermal gradient tube. The gaps between sampling points may contain other interesting information. One may be guided in the selection of samples by visual observation and gamma scans (if available). The change from one structure type to another may or may not be sharply defined. The average size of particles generally decreased toward the cooler end of the TGTs, but sharp discontinuities in size may occur where certain high-concentration elements and compounds are depleted by condensation onto the surfaces. These elements and compounds may also be present in cooler regions, having been transported and deposited as aerosol particles. The thickness of the observed deposits and the composition at different depths into the deposit can provide information on the order in which material was released from the furnace. The calculations of gas composition during the experiment can help to interpret the chemical form of some released elements, although exposure to moist air subsequent to the test can affect some of these (e.g., CsOH) results.

Release of tin during these experiments were generally quite high. (Since there is about 500 kg of tin in an average large LWR, the behavior of the vapor species of tin is an important consideration.) The cladding was fully oxidized by the completion of test HS-2, HS-4, and VI-1, and the fuel was heated essentially isothermally. Under reactor conditions of incomplete oxidation and substantial temperature gradients in the core, tin releases may be much less. Parker has measured up to 3.3% release in core-melt experiments.⁹ Transport of tin occurred throughout the period of the tests, as shown by the concentrations found from all TGTs and filters. Calculations with thermodynamic data on the F*A*C*T system¹⁰ indicate that SnO will form at substantial pressures ($>10^{-4}$ atm) even at hydrogen-to-steam ratios as high as 10^3 . Tin monoxide (SnO) is

probably the form of release and transport, as aerosol and vapor; subsequent oxidation to SnO_2 may have occurred later in the tests as more steam became available. Much of the tin was found as very fine deposits on filters; some alloy formation with platinum in the early part of HS-2 may have occurred, as SnO can easily be reduced to Sn by hydrogen. Phase diagram information (relating to equilibrium bulk mixtures of elements) must be interpreted with care, as a thin layer of one material on another may act as almost any conceivable mixture.

The cesium data from these studies showed only one clear identification of bulk cesium-containing particles, in the steam-starved TGT A portion of test VI-1. Otherwise, cesium was distributed fairly evenly through the TGTs and was an important constituent of aerosol material on the filters. Very porous structures, such as those found on TGT A of VI-1 containing large amounts of cesium, might be susceptible to resuspension in high gas flows, or may be easily dissolved if reflooded. It appears that cesium shows little interaction with platinum; this would not be the case with stainless steel structures.¹¹ The cesium peaks near the exits of all three TGTs in test VI-1 may be due to a relatively volatile molybdate — high levels of molybdenum were found in this region by SSMS.⁷

The control rod alloy included in test HS-4 yielded some particularly interesting structures. The spheres and coalescing-but-frozen "spheres" of silver (HS-4) were clearly liquid at or near the temperature at which they were deposited. Silver also dominated the analysis of much of TGT A and the filters in test HS-4, where previously liquid droplets and finer, possibly partially oxidized aerosol material, were found. The matted layers in TGT A (16 cm) look continuous, as if they had been liquid at one stage. It may be that the structure formed and was knitted together by Cd, In, and Sn; it is clearly not powdery and available for transport. The vaporization and transport of so much silver was due to the horizontal orientation of the furnace trapping the silver in a hot region. It is usually thought that silver and indium will flow from a ruptured control rod to cooler regions,¹² but it is possible that a burst at the top of a control rod while the atmosphere is at high pressure may result in trapping of the liquid alloy in a high-temperature region of the reactor. It would then be possible that silver vapor could escape from the furnace to condense in the TGTs and form the droplets.

Concentrations of indium were found at the inlet end of TGT B (HS-4), where the platinum surface was severely altered. Some evidence of melting was also visible. Indium/platinum alloys with melting points $\sim 1000^\circ\text{C}$ exist throughout the 50 to 100% indium range. The growth or eruption of the platinum surface near this region may be due to expansion of the grains resulting from compound formation. Concentrations of cadmium were not identified unambiguously. Cadmium is by far the most volatile of these three elements and would probably have formed aerosol particles early in the test, which would be deposited in the cooler regions; the high levels of silver have probably prevented the cadmium X-ray signals from being identified, in most cases.

Uranium was released in test HS-2 and may have been released in HS-4. Very small amounts were also found in VI-1 by chemical analysis (~0.03% of inventory). Full cladding oxidation and exposure of the fuel to the gas stream would lead to some UO_2 oxidation to " UO_3 ." This material loses integrity quite rapidly and could be physically transported as particles.¹³ However, the dissolution of the fuel pellets in HS-4, presumably by a combination of reduction and alloying by Zircaloy, stainless steel, and control rod material, may have fixed the UO_2 in the furnace region, as a liquid with a low vapor pressure, even at the highest temperatures. The only positive identification of uranium in these SEM studies was in HS-2, where the X-ray signal could not be confused for that of cadmium. Transport in this case was probably by spallation.

The important fission product, tellurium, was identified at the cooler end of TGT B in test VI-1. Due to the radioactive contamination problems, similar samples from TGT C were not examined. The SSMS analysis confirmed high levels of tellurium at the outlet ends of both TGT B and TGT C in test VI-1. The deposits at the cool ends of all TGTs tended to be very fine particles loosely bound together and to the surface. Thus, no positive identification of shape or size for individual tellurium-containing particles could be made. This material is probably largely deposited aerosol, but calculations of particle behavior in the TGT should be performed. Previous evidence for tin telluride release and transport from the furnace region¹⁴ is not contradicted by these findings; there was no tellurium in TGT A (the cladding was not yet fully oxidized), and the wide range of other materials present in this test may have led to SnTe absorption onto other aerosols and subsequent deposition at the cooler ends of the collection tube, rather than the condensation peak expected at about 600°C.

The behavior of contaminant elements, such as S, Si, and Ca, is of little relevance to a real reactor during the early stages of an accident (fission product release from "intact" fuel). However, some BWR control rods contain borosilicate glass, and later in the accident, core-concrete interactions may allow other elements (e.g., Na, Mg, Al, Si, Ca, K) to become mobilized. Silicon is probably transported from a high-temperature region as SiO , which "disproportionates" to SiO_2 and Si on condensing. Thus, atomic silicon may be available in cooler regions of the apparatus. Silicon monoxide has a vapor pressure of 10^{-4} torr at 1000°C. Some compositions of alloys of Si with Pt and Ni (if stainless steel) exhibit low melting points (<1000°C). In the present work, the platinum whiskers may be a result of interactions with silicon, followed by melting at the inlet end of the TGT. Physical transport of recrystallized fragments could have occurred later in the experiment when the TGTs were cooling down but the gas was still flowing (e.g., VI-2 pretest). In the more complex experiments, however, sulfur has obviously reacted with the platinum-containing whiskers and they were not found dispersed from the hotter regions of the TGTs. Sulfur probably transported as SSi , a relatively volatile species well-known to ceramists, and reacted further after arrival at the platinum surface.

Stainless steel was present in the furnace region of test HS-4 only. The manganese releases were in excess of their proportion in the steel, as expected, at up to 2000°C. Above that, the iron was released strongly; these elements were present throughout the TGT and filters but were major constituents of some very porous and convoluted structures at and around 600°C (TGT B). These may have condensed as small particles in the gas stream and settled onto the surface. The behavior of a stainless steel TGT cannot be inferred from this information. If S and Si levels are restricted, representative information should be obtained from such a tube. It may be worthwhile placing a stainless steel foil inside a platinum TGT (or vice versa) for at least one test such that an exact comparison of effects can be made.

No iodine was detected in any SEM analysis of VI-1. This is probably because of its lower abundance relative to cesium, etc., rather than because it was not there. It would be expected in a broad peak around 500°C, as CsI. Some may be transported as aerosol to the filter surfaces.

The crystalline or glassy structures observed in HS-2 must be due to a combination of interactions. The high levels of tungsten observed here (from the thermocouple) probably mean that these structures were an artifact of the environment. The tungsten probably transported as WO_3 , resulting from steam oxidation of the W/Re wires, which would have oxidized after fracture of the ceramic thermowell. The general level of attack on platinum and stainless steel TGTs is not such that their integrity was threatened. Grain boundary penetration in the steel samples was limited, as shown by the cross sections.

Overall, the surfaces were considerably roughened from their original conditions. This roughness may lead to enhanced holdup of aerosol particles. The size of deposits on the surface generally decreased toward the cooler surfaces; most species have very low vapor pressures at the cooler temperatures and would only have transported that far as aerosols, the smaller ones traveling further. Deposits at the cooler ends were poorly bound to the surface. Redissolution or resuspension of deposited particles would be enhanced by the high surface areas offered by these deposits.

7. CONCLUSIONS AND RECOMMENDATIONS

This report presents the results of preliminary analysis of material that deposited on the thermal gradient tubes during fission product release experiments. The observations of the preliminary examinations are summarized below, along with recommendations for future efforts.

1. The study of material collected in thermal gradient tubes by scanning electron microscopy and energy dispersive X-ray analysis can reveal interesting features. Even quite radioactive samples, up to 0.5 R/h at contact, can be studied without loss of picture quality. However, EDX analysis is effectively prevented by the highest-activity samples.

2. Complex interactions between volatile species and the surface resulted in a wide variety of physical features. The temperature, gas composition, and presence of contaminants all affected the shape and composition of the deposits.
3. The layers in the deposits can reveal information about the sequence of release of material from the fuel.
4. The average size of TGT deposits decreased toward the cooler regions. At the inlet (hottest) end, particles or agglomerates of up to 50 μm were found. At the outlet end, material of $\sim 0.5 \mu\text{m}$ was universally found. The filters were covered with thick layers of very fine ($< 0.1 \mu\text{m}$) aerosol particles.
5. Cesium-containing crystals, probably deposited as CsOH, were found loosely attached to the surface around 600°C in test VI-1; they may be susceptible to resuspension or rapid dissolution.
6. Tin appeared in almost every area analyzed; very high fractions were released. It might not be released in these proportions from a full-scale reactor. Some alloying with platinum was observed, and it appeared to be transported mainly as an aerosol, especially under oxidizing conditions.
7. Uranium releases have been detected; these appeared to be fragments released from the fuel matrix, probably under oxidizing conditions (test HS-2). However, where extensive dissolution occurred in the presence of liquid Zircaloy, etc. (test HS-4), uranium was not released in measurable quantities.
8. The trapping of control rod alloy in high-temperature regions resulted in formation of silver-rich vapors which condensed into liquid droplets, perhaps becoming available to aid in the transport of other materials.
9. Involatile species, such as barium and ruthenium, were not released in large amounts, even at 2450°C. In one experiment (HS-4), the ruthenium segregated into metal beads in the UO_2 matrix.
10. Stainless steel TGTs should be introduced, once they have been tested alongside platinum ones. Furnace design should be modified to prevent excessive releases of contaminants from the ceramic insulation, if possible.
11. The purchase of a new SEM for future work should include microprobe facilities and at least a 30-kV accelerating voltage. Gold coating of active samples should be introduced to minimize the possibility of contamination in the instrument.

8. REFERENCES

1. M. F. Osborne, J. L. Collins, R. A. Lorenz, K. S. Norwood, J. R. Travis, and C. S. Webster, Data Summary Report for Fission Fission Product Release Test HI-6, NUREG/CR-4043 (ORNL/TM-9443), Oak Ridge Natl. Lab., September 1985.
2. K. S. Norwood, An Assessment of Thermal Gradient Tube Results from the HI Series of Fission Product Release Tests, NUREG/CR-4105 (ORNL/TM-9506), Oak Ridge Natl. Lab., March 1985.
3. J. Schreibermaier, V. Matschoss, H. Albrecht, and A. Mack, Herstellung von Kernbrennstoff mit Simuliertem Abbrand (Fission) an der Anlage FIFA, KfK-2991, Kernforschungszentrum Karlsruhe, June 1980.
4. M. F. Osborne, J. L. Collins, and R. A. Lorenz, Highlights Report for Fission Product Release Tests of Simulated LWR Fuel, ORNL/NRC/LTR-85/1, Oak Ridge Natl. Lab., February 1985.
5. T. Yamashita, Steam Oxidation of Zircaloy Cladding in the ORNL Fission Product Release Tests, NUREG/CR-4777 (ORNL/TM-10272), Oak Ridge Natl. Lab., in preparation.
6. W. Dienst, P. Hofmann, and D. K. Kerwin-Peck, "Chemical Interactions Between CO_2 and Zircaloy-4 from 1000 to 2000°C," Nucl. Technol. 65(1), 109-24 (1984).
7. M. F. Osborne, J. L. Collins, R. A. Lorenz, and T. Yamashita, Highlights Report for Fission Product Release Test VI-1, ORNL/NRC/LTR-86/7, Oak Ridge Natl. Lab., March 1986.
8. M. F. Osborne, J. L. Collins, P. A. Haas, R. A. Lorenz, J. R. Travis, and C. S. Webster, Design and Final Safety Analysis Report for Vertical Furnace Fission Product Release Apparatus in Hot Cell B, Building 4501, NUREG/CR-4332 (ORNL/TM-9720), Oak Ridge Natl. Lab., January 1986.
9. G. W. Parker, personal communication at ORNL, 1986.
10. F*A*C*T is a copyrighted product (computer program) of THERMFACT Ltd., 447 Berwick Ave., Mount Royal, Quebec, Canada, H3R1Z8.
11. B. R. Bowsher, S. Dickinson, and A. L. Nichols, High Temperature Studies of Simulant Fission Products: Part I, Vapor Deposition and Interaction of Caesium Iodide, Caesium Hydroxide, and Tellurium with Stainless Steel, AEEW-R1697, July 1983.

12. J. P. Mitchell, A. L. Nichols, and J. A. H. Simpson, "The Characterization of Ag-In-Cd Control Rod Aerosols Generated at Temperatures Below 1500°C," in Proceedings of the CSNI Specialist Meeting on Nuclear Aerosols in Reactor Safety, Karlsruhe, Federal Republic of Germany, Sept. 4-6, 1985, KfK 3800, CSNI 95, February 1985.
13. T. Maatsui and K. Naito, "Vaporization Study on UO₂ and (U_{1-y}Nb_y)O_{2+x} by Mass-Spectrometric Method," J. Nucl. Mater. 136, 69-77 (1985).
14. J. L. Collins, M. F. Osborne, and R. A. Lorenz, "Behavior of Fission Product Tellurium Under Severe Accident Conditions," in Proceedings of the International ANS/ENS Topical Meeting on Thermal Reactor Safety, San Diego, Cal., Feb. 2-6, 1986, ANS Order No. 700106 (ISBN Order No. 0-89448-121-5), February 1986.

NUREG/CR-4778
 ORNL/TM-10273
 Dist. Category R-3

INTERNAL DISTRIBUTION

- | | |
|----------------------|---------------------------------|
| 1. E. C. Beahm | 15. J. R. Travis |
| 2. J. T. Bell | 16. C. S. Webster |
| 3. D. O. Campbell | 17. A. L. Wright |
| 4. J. L. Collins | 18. R. P. Wichner |
| 5. S. R. Daish | 19-23. S. J. Wisbey |
| 6. J. R. Hightower | 24. R. G. Wymer |
| 7. T. S. Kress | 25. Central Research Library |
| 8. T. B. Lindemer | 26. ORNL-Y-12 Technical Library |
| 9. R. A. Lorenz | Document Reference Section |
| 10-12. M. F. Osborne | 27-28. Laboratory Records |
| 13. G. W. Parker | 29. Laboratory Records, ORNL RC |
| 14. M. G. Stewart | 30. OKNL Patent Section |

EXTERNAL DISTRIBUTION

31. Office of Assistant Manager for Energy Research and Development, ORO-DOE, P.O. Box X, Oak Ridge, TN 37831
32. Director, Division of Reactor Safety Research, U.S. Nuclear Regulatory Commission, Washington, DC 20555
- 33-34. Technical Information Center, DOE, Oak Ridge, TN 37831
35. Division of Technical Information and Document Control, U.S. Nuclear Regulatory Commission, Washington, DC 20555
36. L. K. Chan, U.S. Nuclear Regulatory Commission, Fuel Systems Research Branch, Division of Accident Evaluation, U.S. Nuclear Regulatory Commission, Washington, DC 20555
37. K. S. Norwood, Chemical Technology Division, R10.5, AERE Harwell, Didcot, OXON OX11, ORA, England
38. T. Yamashita, Nuclear Fuel Chemistry Laboratory, Department of Chemistry, Japan Atomic Energy Research Institute, Tokai-mura, Naka-gun, Ibaraki-ken, 319-11, Japan
- 39-288. Given distribution as shown in Category R-3 (NTIS - 10)

| | | |
|--|---|--|
| NRC FOR # 335 (2-84) NRCM 1102 3201, 3202 SEE INSTRUCTIONS ON THE REVERSE | U.S. NUCLEAR REGULATORY COMMISSION BIBLIOGRAPHIC DATA SHEET | 1 REPORT NUMBER (Assigned by TIDC, add Vol. No., if any) NUREG/CR-4778 ORNL/TM-10273 |
| 2 TITLE AND SUBTITLE Preliminary Studies of the Morphology of Thermal Gradient Tube Deposits from Fission Product Release Experiments | 3 LEAVE BLANK | 4 DATE REPORT COMPLETED MONTH: December YEAR: 1986 |
| 5 AUTHOR(S) S. J. Wisbey | 6 DATE REPORT ISSUED MONTH: February YEAR: 1988 | 8 PROJECT/TASK/WORK UNIT NUMBER |
| 7 PERFORMING ORGANIZATION NAME AND MAILING ADDRESS (Include Zip Code) Oak Ridge National Laboratory Post Office Box X Oak Ridge, Tennessee 37831 | 9 PIN OR GRANT NUMBER B0127 | 11a TYPE OF REPORT NUREG |
| 10 SPONSORING ORGANIZATION NAME AND MAILING ADDRESS (Include Zip Code) Division of Accident Evaluation Office of Nuclear Regulatory Commission U.S. Nuclear Regulatory Commission Washington, D.C. 20555 | 11b PERIOD COVERED (Include 0000) October 1985 - September 1986 | 12 SUPPLEMENTARY NOTES |
| 13 ABSTRACT (200 words or less) <p>Sections of thermal gradient tubes and deposits from filters used as collectors in several fission product release tests at ORNL have been examined by scanning electron microscopy with elemental identification by energy dispersive X-ray analysis. Shape, size, and composition of the deposits are reported; correlations with experimental conditions such as gas composition and temperature, as well as with independent analyses, have been made where possible. A wide variety of shapes and structures, apparently dependent on the deposition temperature, were photographed and elemental analyses were recorded. Although some fission products (Cs, Ba, Ag) were detected, structural and impurity elements (Sn, Si, S, W, Pt) were predominant in most cases. Recommendations for analytical procedures and handling of similar samples are made for the future.</p> | | |
| 14 DOCUMENT ANALYSIS - KEYWORDS DESCRIPTORS Energy dispersive X-ray Fission products Scanning electron microscopy Thermal gradient tube 15 IDENTIFIERS OPEN ENDED TERMS | 15 AVAILABILITY STATEMENT NTIS | 16 SECURITY CLASSIFICATION (This page) <u>Unclassified</u> (This report) |
| | 17 NUMBER OF PAGES 49 | 18 PRICE |

120555078877 1 14N1R3
US NRC-OARM-ADM
DIV OF PUB SVCS
POLICY & PUB MGT BR-PDR NUREG
W-537
WASHINGTON DC 20555